

**UCLA**

**UCLA Electronic Theses and Dissertations**

**Title**

Amplification-Free Detection of 16S rRNA for Next Generation Point-of-Care Diagnostics

**Permalink**

<https://escholarship.org/uc/item/0q1207sz>

**Author**

Zheng, Zhenrong

**Publication Date**

2022

Peer reviewed|Thesis/dissertation

UNIVERSITY OF CALIFORNIA

Los Angeles

Amplification-Free Detection of 16S rRNA for Next Generation Point-of-Care Diagnostics

A dissertation submitted in partial satisfaction of the  
requirements for the degree of Doctor of Philosophy  
in Chemical Engineering

by

Zhenrong Zheng

2022



## ABSTRACT OF THE DISSERTATION

Amplification-Free Detection of 16S rRNA for Next Generation Point-of-Care Diagnostics

by

Zhenrong Zheng

Doctor of Philosophy in Chemical Engineering

University of California, Los Angeles, 2022

Professor Harold G. Monbouquette, Chair

The ongoing COVID-19 global pandemic has highlighted the need for point-of-care (POC) testing to monitor public health threats and to provide timely healthcare to patients. POC testing involves performing a diagnostic test that produces a rapid and reliable result outside the laboratory at the point of first contact between patients and healthcare professionals. In previous work, our group successfully demonstrated a novel nucleic acid (NA) sensing method based on simple pore blockage. In our approach, uncharged peptide nucleic acid (PNA) probes are conjugated to carboxyl-functionalized microspheres to form nearly neutral complexes that do not exhibit electrophoretic movement in an electric field. When the probe-bead conjugates capture the target NA, they gain negative charge and therefore become mobile in the presence of an electric field. If the probe-bead conjugate with hybridized target NA is directed to a smaller diameter pore in a thin

glass membrane, it will at least partially block it resulting in a sustained drop in ionic current, which serves as the detection signal. We achieved a limit of detection of 1 aM ( $10^{-18}$  M) *E. coli* 16S rRNA with this simple scheme, yet this approach required laboratory-based manipulations and a turnaround time of 10 hours. In this dissertation, we present our work to reduce the total assay time and complexity so that this technology can meet the criteria for POC testing.

To reduce the lengthy sampling time, alkaline lysis followed by simple filtration was explored to accelerate the NA isolation process. In addition, kinetically enhanced hybridization was accomplished by passing NA samples through a compact bed of charge neutral peptide nucleic acid (PNA) capture probes conjugated to submicron polystyrene beads. With these two improvements, we shortened the lab-based process time to 30 minutes and achieved a limit of detection (LOD) of 100 zM ( $10^{-19}$  M) *E. coli* 16S rRNA. However, work with *E. coli* spiked in sterile, pooled human urine suggested that a subsequent cleanup is needed for alkaline extraction in complex media. Rapid commercial RNA extraction kits therefore were used to achieve more consistent results in later work. To evaluate the capability of our technology to detect an important pathogen in complex media, kinetically enhanced hybridization was used to capture the 16S rRNA of *Neisseria gonorrhoeae* spiked in human urine. Based on 44 test runs, the ability to detect *N. gonorrhoeae* over the range of 10 to 100 CFU/mL spiked in human urine was demonstrated

successfully with sensitivity and specificity of ~98% and ~100%, respectively. No false positives were observed for the control group of representative background flora at 1000 CFU/mL.

To further improve our technology for POC applications, we integrated the nanopore detector with the lateral flow assay (LFA) format. In this approach, an extracted NA sample quickly flows along the LFA membrane by capillary action and hybridizes with preloaded PNA-bead conjugates. The resulting conjugates that are hybridized with negatively charged target RNA therefore move toward and block the smaller glass nanopore under the influence of an external electric field. The detection of 10 aM *E. coli* 16S rRNA against 10 fM *P. putida* 16S rRNA within 15 minutes has been successfully demonstrated. Finally, our LFA format device rapidly detected *E. coli* at 10 CFU/mL against a one-million-fold background of viable *P. putida*. With further improvements in sensitivity and reliability, this simple, rapid, and inexpensive amplification-free technology may be promising for widespread diagnostic usage in defense of public health.

The dissertation of Zhenrong Zheng is approved.

Dante A. Simonetti

Yi Tang

Jacob J. Schmidt

Harold G. Monbouquette, Committee Chair

University of California, Los Angeles

2022

## Table of Contents

<b>Chapter 1: Introduction to point-of-care (POC), amplification-free nucleic acid detection.....</b>	<b>1</b>
1.1 Motivation.....	1
1.2 Current detection methods .....	1
1.3 Novel platform of nanopore based sequence specific detection of 16S rRNA.....	2
1.4 References .....	4
<b>Chapter 2: Nucleic acid amplification-free detection of DNA and RNA at ultralow concentration.....</b>	<b>7</b>
2.1 Introduction.....	7
2.2 Optical methods.....	10
2.2.1 Förster resonance energy transfer (FRET) .....	10
2.2.2 Bio-barcode method .....	11
2.2.3 Quantum dot fluorescence .....	11
2.2.4 Surface enhanced Raman spectroscopy (SERS) and surface plasmon resonance (SPR) .....	12
2.2.5 Darkfield microscopy .....	13
2.3 Electrochemical/Electronic methods.....	14
2.3.1 Mass spectrometry (MS) .....	14
2.3.2 Constant potential amperometry.....	15
2.3.3 Voltammetry.....	16
2.3.4 Electrochemical impedance spectroscopy (EIS) .....	19
2.3.5 Field effect transistors (FETs) .....	19
2.3.6 Piezoelectric plate sensor.....	21
2.4 Nanopore sensors .....	21
2.5 Conclusion and outlook.....	22
2.6 References .....	24
<b>Chapter 3: Simplified NA extraction and enhanced kinetic hybridization for amplification-free, sequence-specific 16S rRNA detection at 100 zM.....</b>	<b>31</b>
3.1 Introduction.....	32
3.2 Materials and methods .....	34
3.2.1 Reagents.....	34



3.2.2 Coupling PNA probe to microspheres.....	34
3.2.3 Cell culturing.....	35
3.2.4 RNA extraction.....	36
3.2.5 Hybridization of RNA to PNA-bead conjugate.....	37
3.2.6 Sample detection.....	38
3.3 Results and discussion.....	39
3.4 Conclusion.....	43
3.5 References.....	44
<b>Chapter 4: Detection of <i>E. coli</i> spiked in sterile pooled human urine .....</b>	<b>47</b>
4.1 Introduction.....	47
4.2 Method and materials.....	48
4.3 Results and Discussion.....	48
4.4 Conclusion.....	52
4.5 Reference.....	52
<b>Chapter 5: An amplification-free, 16S rRNA test for <i>Neisseria gonorrhoeae</i> in urine.....</b>	<b>54</b>
5.1 Introduction.....	55
5.2 Methods and materials.....	57
5.2.1 Reagents.....	57
5.2.2 Detector assembly.....	57
5.2.3 Coupling PNA probe to microspheres.....	58
5.2.4 RNA extraction.....	59
5.2.5 Hybridization of RNA to PNA-bead conjugates.....	60
5.2.6 Sample detection.....	60
5.3 Results and Discussion.....	61
5.4 Conclusions.....	64
5.5 References.....	65
<b>Chapter 6: Amplification-free detection of 16S rRNA using a glass chip detector integrated into the lateral flow assay format .....</b>	<b>67</b>
6.1 Introduction.....	68
6.2 Method and Materials.....	70
6.2.1 Reagents.....	70

6.2.2 Coupling PNA probe to microspheres .....	70
6.2.3 Cell culturing and counting .....	71
6.2.4 RNA extraction.....	72
6.2.5 Lateral flow assay system assembly and sample detection .....	73
6.3 Result and Discussion .....	75
6.4 Conclusion.....	79
6.5 Reference.....	80
<b>Chapter 7: Recommendations for future work.....</b>	<b>82</b>
7.1 Cell lysis.....	82
7.2 Develop a syringe type device for NA extraction .....	83
7.3 Improve the LOD and stability.....	84
7.4 References .....	85
<b>Appendix A: PNA-beads preparation.....</b>	<b>86</b>
<b>Appendix B: Cell culturing and counting.....</b>	<b>87</b>
B.1 Culture <i>E. coli</i> and <i>P. putida</i> .....	87
B.2 Count viable <i>E. coli</i> and <i>P. putida</i> .....	87
B.3 Culture and count <i>N. gonorrhoeae</i> .....	88
<b>Appendix C: Spike sterilized pool human urine with bacterial culture.....</b>	<b>89</b>
C.1 <i>E. coli</i> and <i>P. putida</i> .....	89
C.2 <i>N. gonorrhoeae</i> .....	89
<b>Appendix D: RNA extraction.....</b>	<b>90</b>
D.1 Qiagen RNeasy (Chapter 2) .....	90
D.2.1 Alkaline Extraction (cell pellet, Chapter 2).....	91
D.2.2 Alkaline Extraction (urine sample, Chapter 3).....	91
D.3 Direct-zol RNA extraction Kit .....	92
<b>Appendix E: Kinetically Enhanced Hybridization.....</b>	<b>93</b>
<b>Appendix F.....</b>	<b>94</b>
F.1 Lateral flow strip assembly .....	94
F.2 Glass chip assembly .....	95
F.3 Whole system assembly .....	96
F.4 Detection .....	97

## LIST OF FIGURES

Figure 2.1. Detection of microRNA by surface plasmon resonance using triangular Au nanoparticles (see text)[20].....	14
Figure 2.2. DNA detection by constant potential amperometry using Pt-labeled signal oligonucleotides and Pt-catalyzed, H <sub>2</sub> O <sub>2</sub> electroreduction (see text)[28].....	17
Figure 2.3. microRNA detection using carbon nanotube field effect transistors functionalized with the Carnation Italian ringspot virus p19 protein (see text)[39].....	21
Figure 3.1. Schematic of kinetic enhanced hybridization between PNA beads and the target RNA .....	38
Figure 3.2 Glass chip and detector assembly. a) The 1 cm × 1 cm chip with ~1 μm-thick membrane and pore in the center. b) Micrograph of the ~1 μm-thick membrane at the chip center. c) Micrograph of the ~500 nm pore at the center of the glass membrane. d) The glass chip sandwiched between Teflon chambers (6 mm × 6 mm × 8 mm). .....	39
Figure 3.3. PNA-beads tests with Qiagen extraction kit and over-night hybridization. a) shows repeated, consistent current drops using in a concentration of 100 zM <i>E. coli</i> 16S rRNA, and b) shows no current drop occurred with 10 zM <i>E. coli</i> 16S rRNA. ....	40
Figure 3.4. I) 820-nm carboxylic beads tests with alkaline extraction and over-night hybridization a) shows repeated, consistent current drop in a concentration of 100 zM of <i>E. coli</i> 16S rRNA, and b) shows that no current drop occurred for 10 fM of <i>P. putida</i> 16S rRNA. II) 820-nm carboxylic beads tests with alkaline extraction and kinetic enhanced hybridization c) shows repeated, consistent current drop in a concentration of 100 zM of <i>E. coli</i> 16S rRNA, and d) shows that no current drop occurred for 100 fM of <i>P. putida</i> 16S rRNA. ....	43
Figure 4.1. 820-nm carboxylic beads tests with alkaline extraction and kinetic enhanced hybridization a) shows unrepeatable permanent current drops for 10 CFU/mL of <i>E. coli</i> in sterilized human urine, and b) shows a false positive for 1000 CFU/mL of <i>P. putida</i> in sterilized human urine. ....	49
Figure 4.2. Blank human urine test shows repeatable permanent current drops. ....	50
Figure 4.3. 820-nm carboxylic beads tests with alkaline extraction, lipase treatment, and kinetic enhanced hybridization a) shows repeated, consistent current drops for 10 CFU/mL of <i>E. coli</i> in sterilized human urine, and b) shows that no false positive for 1000 CFU/mL of <i>P. putida</i> in sterilized human urine.....	51

Figure 5.1. Glass chip and detector assembly. a) The 1 cm × 1 cm chip with ~1 μm-thick membrane and pore in the center. b) Micrograph of the ~1 μm-thick membrane at the chip center. c) Micrograph of the ~500 nm pore at the center of the glass membrane. d) The glass chip sandwiched between Teflon chambers (6 mm × 6 mm × 8 mm)..... 58

Figure 5.2. Detector current response to the presence of target *N. gonorrhoeae* 16S rRNA and the lack of response to RNA extracted from background bacterial flora alone. a) Reproducible, sustained current signal step changes down in response to the presence of PNA-beads with hybridized target rRNA extracted from *N. gonorrhoeae* at 100 CFU/mL in human urine. b) No current signals in response to the presence of PNA-beads with hybridized with RNA extracted from background bacterial flora spiked at 1000 CFU/mL in human urine (negative control). The applied voltage for detection events was 1.5 V. After a sustained current signal of at least 20 sec, the voltage polarity was reversed temporarily to -1.5 V for at least several seconds to drive bead complexes a short distance away from the pore mouth before demonstrating signal reversibility by reimposing a potential of 1.5 V..... 62

Figure 6.1. a) A microfabricated 1 cm × 1 cm glass chip. b) SEM image of ~0.25 mm<sup>2</sup>, 1 μm-thick membrane in the center of glass chip by wet etch. c) SEM image of ~500 nm nanopore bored in the center of etched membrane using FIB.[11]..... 74

Figure 6.2. Schematic diagram for the lateral flow assay with integrated nanopore detector. Not to scale..... 75

Figure 6.3. PNA-bead tests with LFA format nanopore detector: a) Repeated, consistent current drops for *E. coli* PNA-beads hybridized with 10 aM of target *E. coli* 16S rRNA, b) No current drop for *E. coli* PNA-beads hybridized with 10 fM control *P. putida* 16S rRNA, c) Repeated, consistent current drops for *E. coli* PNA-beads hybridized with 10 aM of *E. coli* 16S rRNA against 10 fM control *P. putida* 16S rRNA, and d) Repeated, consistent current drops for *E. coli* PNA-beads hybridized with RNA extracted from a mixture of 10 CFU/mL of *E. coli* and 10<sup>6</sup> CFU/mL of *P. putida*. ..... 79

Figure 7.1. Proposed scheme for all-in-one cell lysis device ..... 83

Figure 7.2. a) Proposed cartridge to replace the backing card, not to scale b) 3-D printed cartridge with plastic clips ..... 84

Figure F.1. Lateral flow membrane strip, not to scale. Point A is where PNA-modified beads are loaded and dried (see below). ..... 94

Figure F.2. Glass chip with PDMS films attached, not to scale. .... 95

Figure F.3. Detection system, not to scale ..... 96

## LIST OF TABLES

Table 3.1. RNA extraction time, yield, estimated 16S rRNA concentration and purity using the Qiagen kit compared to the alternate alkaline lysis/neutralization/filtration approach. ....	41
Table 4.1. Comparison of RNA purity between pelleted bacterial culture (Case A) and bacteria-urine mixtures (Case B) using alkaline extraction.....	49
Table 5.1. Complete summary of <i>N. gonorrhoeae</i> detection data over a concentration range of 10-100 CFU/mL in human urine as well as negative control data (see text). ....	63
Table 6.1. Summary of results where <i>E. coli</i> PNA-beads were hybridized separately with <i>E. coli</i> RNA (target) and <i>P. putida</i> RNA (negative control).....	78
Table 6.2. Summary of results where <i>E. coli</i> PNA-beads were hybridized with mixed <i>E. coli</i> and <i>P. putida</i> RNA; and where <i>E. coli</i> PNA-beads were hybridized with RNA extracted from mixtures of cultures of <i>E. coli</i> and <i>P. putida</i> .....	78

## Acknowledgments

First, I would like to express my deepest thanks to my Ph.D. advisor, Professor Harold G. Monbouquette for the guidance and support throughout my graduate study and research. I have learned how to better organize my research plan, analyze preliminary results, and identify and resolve problems. In addition, I would like to thank my committee members, Professor Dante Simonetti, Professor Yi Tang, and Professor Jacob J. Schmidt for their valuable questions and suggestions.

I would also thank to the collaborators on the nucleic acid detection project. Professor Jacob J. Schmidt always provided insightful ideas to solve challenging problems. Dr. Omai B. Garner and Dr. Sukantha Chandrasekaran from UCLA Pathology and Laboratory Medicine provided help in culturing pathogenic species for testing.

I also appreciate my lab mates, Dr. Allison M. Yorita, Dr. Bonhye Koo, Dr. I-wen (Brenda) Huang, Dr. Mac Clay, Yan Cao and Dima Ruckodanov. Dr. Yorita and Dr. Koo guided me with valuable lessons in starting the nucleic acid detection project, and Dr. Huang shared experience and tips with me on nanofabrication. Dr. Mac Clay helped me understand the mathematical simulations better. I have worked closely with Yan Cao on the nucleic acid detection project, and I really thank him for the constructive discussions and work in these very intense academic years.

Lastly, I would be remiss in not mentioning my family, especially my parents and spouse. Their unconditional support and encouragement have kept my passion and motivation alive during my entire graduate school career.

## Vita

- 2012-2015      *B.S., Chemical and Biomolecular Engineering*  
University of California, Los Angeles  
Los Angeles, CA
- 2016-2022      *Graduate Student Researcher, Department of Chemical and Biomolecular Engineering*  
University of California, Los Angeles  
Los Angeles, CA
- 2016-2022      *Teaching Assistant, Department of Chemical and Biomolecular Engineering*  
University of California, Los Angeles  
Los Angeles, CA

## PUBLICATION AND PRESENTATIONS

**Zhenrong Zheng** and Harold G. Monbouquette, “Simplified NA extraction and enhanced kinetic hybridization for amplification-free, sequence-specific 16S rRNA detection at 100 zM,” *In preparation*

**Zhenrong Zheng**, Yan Cao, Sukantha Chandrasekaran, Jacob J. Schmidt, Omai Garner, and Harold G. Monbouquette, “An amplification-free, 16S rRNA test for *Neisseria gonorrhoeae* in urine,” *In preparation*

**Zhenrong Zheng**, Yan Cao, Jacob J. Schmidt, and Harold G. Monbouquette, “Amplification-free detection of 16S rRNA using a glass chip detector integrated into the lateral flow assay format,” *In preparation*

**Zhenrong Zheng**, Yan Cao, Sukantha Chandrasekaran, Jacob Schmidt, Omai Garner, and Harold G. Monbouquette, “Amplification-Free Detection of 16S rRNA for Point-of-Care Gonorrhea Diagnosis,” *ACS Spring 2022*, Division of Biochemical Technology, San Diego, CA, 2022 (Oral Preparation)

Yan Cao, **Zhenrong Zheng**, and Harold G. Monbouquette, “Nucleic acid amplification-free detection of DNA and RNA at ultralow concentration,” *Curr Opin Biotechnol*, 2021. **71**: p. 145-150.

# **Chapter 1: Introduction to point-of-care (POC), amplification-free nucleic acid detection**

## **1.1 Motivation**

Sequence specific nucleic acid detection can be applied widely in numerous fields such as disease diagnosis, patient screening during epidemics, and detection of pathogens in food and water. The ongoing COVID-19 pandemic highlighted the need glaringly apparent for rapid, convenient, inexpensive, sensitive and reliable disease diagnostics. If a diagnostic device is intended for widespread use, it should be easy to operate and interpret, and preferably in a point-of-care (POC) setting. Further, it must be rapid, as it has been observed that a significant portion of the patient population will not wait in a clinic more than 20 minutes for a test result.[1, 2] Finally, ideal tests should be inexpensive, especially if tests are to be repeated at high frequency for each individual, such as during a pandemic; and if the technology is to be made available to developing countries where inefficient disease diagnosis leads to 95% of deaths.[3]

## **1.2 Current detection methods**

Currently, nucleic acid amplification tests (NAATs) appear to provide the best combination of low detection limit and accuracy relative to conventional binding assays such as immunoassays. [4, 5] However, since most NAATs rely on polymerase chain reaction (PCR) to amplify target nucleic acid (NA) in a sample, the process requires high purity NA isolation, precise temperature control, integration with labeled amplicon detection, and perishable reagents including polymerase, primers, and nucleotides. These complexities of NAATs makes them less favorable for POC applications.



Over the past few years, many remarkable works with NA amplification-free detection have been reported based on transduction mechanisms to convert selective hybridization events into detectable signals, such as optical signals or electrochemical signals. For example, oligonucleotide probe-modified gold nanoparticles are widely applied in optical methods to visualize the binding of target NAs.[6-8] Electrochemical approaches, with greater diversity, can involve constant potential amperometry (CPA), voltammetry, and field effect transistors (FETs).[9-14] In electrochemical approaches, current and potential are recorded to analyze the NA capture event. These remarkable approaches can selectively detect NAs at the single digit attomolar level or lower. However, the need for expensive analytical equipment, special labels, or lengthy assay time makes them less favorable for development of inexpensive, handheld POC diagnostics.

### **1.3 Novel platform of nanopore based sequence specific detection of 16S rRNA**

Our novel platform method for NA detection is a nanopore based approach for detection of the sequence-specific 16S rRNA of bacterial pathogens by utilizing complementary peptide nucleic acid (PNA), an uncharged polyamide analog to DNA/RNA. In our system, PNA is covalently bound to carboxyl-functionalized polystyrene microbeads to form charge neutral, bead to PNA probe conjugates. When the neutral PNA-microbead conjugates hybridize with target rRNA, they gain negative charge and therefore exhibit mobility in an electric field. If the complex is directed to a smaller diameter pore in a glass membrane, it will at least partially block it, resulting in a sustained drop in ionic current thereby signaling the presence of the target rRNA.

In a previous study, our group successfully demonstrated detection of 1 attomolar *E. coli* 16S rRNA against 10 femtomolar *P. putida* 16S rRNA. [15] However, it took about 10 hours to complete sample treatment, including RNA extraction and hybridization. In pursuit of POC device development, it is necessary to investigate a faster approach for sample preparation. Since our

system did not involve any NA amplification steps, we hypothesized that there is no need for extensive NA purification through NA adsorption, washing and elution steps to remove inhibitors of polymerases. Therefore, we proposed to lyse bacterial cells with high pH buffer followed by a simple cleanup with filtration. We also anticipated enhancing hybridization kinetics by creating more interfacial contact between PNA-beads and target RNA.

In the meantime, it is important for us to perform tests with clinical or at least mock clinical specimens. Our goal was detection of *N. gonorrhoeae* in mock clinical samples based on recognition of the species-specific 16S rRNA. *N. gonorrhoeae* is the gram-negative diplococcus bacterium responsible for the second most common notifiable communicable disease in the US. *E. coli* was first spiked into sterile human urine to optimize our system. Next, our system was used to examine *N. gonorrhoeae* in sterilized pooled human urine. A significant number of positive and negative samples was tested to determine sensitivity and specificity. A competitive diagnostic system should provide sensitivity and specificity of  $\geq 95\%$ .

Finally, since our ultimate goal is to develop an inexpensive, handheld, and robust device for NA-based detection within 15 minutes. Our nanopore detector must be integrated with cell lysis, RNA extraction, and target rRNA hybridization to PNA probes. Lateral flow assay (LFA) technology provides an attractive approach to integrate our nanopore detector. In LFAs, sample can be easily carried by capillary flow through a strip of membranes, which potentially avoids the need for any installation of complicated valves and pumps. This technology has been applied widely for inexpensive POC immunoassays such as the well-known home pregnancy test. [16-18]

## 1.4 References

1. Atkinson, L.M., et al., *'The waiting game': are current chlamydia and gonorrhoea near-patient/point-of-care tests acceptable to service users and will they impact on treatment?* Int J STD AIDS, 2016. **27**(8): p. 650-5.
2. Hsieh, Y.H., et al., *Perceptions of an ideal point-of-care test for sexually transmitted infections--a qualitative study of focus group discussions with medical providers.* PLoS One, 2010. **5**(11): p. e14144.
3. Jayamohan, H., H.J. Sant, and B.K. Gale, *Applications of microfluidics for molecular diagnostics.* Methods Mol Biol, 2013. **949**: p. 305-34.
4. Cristillo, A.D., et al., *Point-of-Care Sexually Transmitted Infection Diagnostics: Proceedings of the STAR Sexually Transmitted Infection-Clinical Trial Group Programmatic Meeting.* Sex Transm Dis, 2017. **44**(4): p. 211-218.
5. Lui C, C.N., Batt CA, *Nucleic Acid-based Detection of Bacterial Pathogens Using Integrated Microfluidic Platform Systems.* Sensors (Basel), 2009. **9**: p. 3713-3744.
6. Nam, J.M., S.I. Stoeva, and C.A. Mirkin, *Bio-bar-code-based DNA detection with PCR-like sensitivity.* J Am Chem Soc, 2004. **126**(19): p. 5932-3.
7. Taton, T.A., C.A. Mirkin, and R.L. Letsinger, *Scanometric DNA array detection with nanoparticle probes.* Science, 2000. **289**(5485): p. 1757-60.
8. Thaxton, C.S., et al., *A bio-bar-code assay based upon dithiothreitol-induced oligonucleotide release.* Anal Chem, 2005. **77**(24): p. 8174-8.
9. Spain, E., et al., *Detection of sub-femtomolar DNA based on double potential electrodeposition of electrocatalytic platinum nanoparticles.* Analyst, 2013. **138**(15): p. 4340-4.

10. Kim YJ, J.J., Li H, Yampara-Iquise H, Zheng G, Carson CA, Cooperstock M, Sherman M, Yu Q, *Three-dimensional (3-D) microfluidic-channel-based DNA biosensor for ultrasensitive electrochemical detection*. Journal of Electroanalytical Chemistry, 2013. **702**: p. 72-78.
11. Chen CP, G.A., Lu CY, Chen TY, Kuo CC, Chen RS, Tu WH, Fischer WB, Chen KH, Chen LC, *Ultrasensitive in situ label-free DNA detection using a GaN nanowirebased extended-gate field-effect-transistor sensor*. Anal Chem, 2011. **83**: p. 1938-1943.
12. Li, C., et al., *One-Step Modification of Electrode Surface for Ultrasensitive and Highly Selective Detection of Nucleic Acids with Practical Applications*. Anal Chem, 2016. **88**(15): p. 7583-90.
13. Hu, Q., et al., *Electrochemical DNA Biosensing via Electrochemically Controlled Reversible Addition-Fragmentation Chain Transfer Polymerization*. ACS Sens, 2019. **4**(1): p. 235-241.
14. Ramnani P, G.Y., Ozsoz M, Mulchandani A, *Electronic detection of microRNA at attomolar level with high specificity*. Anal Chem, 2013. **85**: p. 8061-8064.
15. Koo, B., et al., *Amplification-free, sequence-specific 16S rRNA detection at 1 aM*. Lab Chip, 2018. **18**(15): p. 2291-2299.
16. Bishop, J.D., et al., *Sensitivity enhancement in lateral flow assays: a systems perspective*. Lab Chip, 2019. **19**(15): p. 2486-2499.
17. Huang, D., et al., *Microfluidic Ruler-Readout and CRISPR Cas12a-Responded Hydrogel-Integrated Paper-Based Analytical Devices (muReaCH-PAD) for Visible Quantitative Point-of-Care Testing of Invasive Fungi*. Anal Chem, 2021. **93**(50): p. 16965-16973.

18. Fridley GE, H.C., Oza SB, Yager P, *The evolution of nitrocellulose as a material for bioassays*. MRS Bulletin, 2013. **38**: p. 326–330.

## **Chapter 2: Nucleic acid amplification-free detection of DNA and RNA at ultralow concentration**

Chapter 2 is a manuscript published with the following citation:

Cao, Y., Z. Zheng, and H.G. Monbouquette, *Nucleic acid amplification-free detection of DNA and RNA at ultralow concentration*. *Current Opinion in Biotechnology*, 2021. **71**: p. 145-150.

### **Abstract**

The broad spectrum of approaches for nucleic acid amplification-free detection of DNA and RNA at single-digit attomolar ( $10^{-18}$  M) concentration and lower is reviewed. These low concentrations correspond roughly to the most clinically desirable detection range for pathogen-specific nucleic acid as well as the detection limits of commercially available, nucleic acid amplification tests based primarily on polymerase chain reaction (PCR). The need for more rapid and inexpensive, yet still highly accurate tests, has become evident during the pandemic. It is expected that publication of reports describing improved tests will accelerate soon, and this review covers the wide variety of detection methods based on both optical and electrical measurements that have been conceived over recent years, enabled generally by the advent of nanotechnology.

### **2.1 Introduction**

The ongoing COVID-19 pandemic and the realization that this public health crisis likely will not be the last of its kind has made the need glaringly apparent for rapid, convenient, inexpensive, sensitive and reliable disease diagnostics. A clinical sample taken for testing gives a “snapshot” of an individual’s disease state of steadily diminishing value with time during a pandemic, and most people, even in developed countries, have access only to testing regimens with a turnaround time of a day or more. Of course, there are many other microbial and viral pathogens that are tested for at high volume (*e.g.*, influenza, Group A Streptococcus, respiratory

syncytial virus, gonorrhoea, chlamydia, *etc.*), and it has been observed that a significant portion of the patient population will not wait in a clinic more than 20 minutes for a test result after giving a sample.[1,2] If a diagnostic device is intended for widespread use, it should accept a conveniently obtained clinical sample (*e.g.*, saliva, nasal swab, urine) and be easy to operate and interpret, preferably in a point-of-care (POC) setting. Further, it should be inexpensive, especially if tests are to be repeated at high frequency for each individual, such as during a pandemic; and if the technology is to be made available to those in developing countries where inefficient disease diagnosis leads to 95% of deaths.[3] Ideally, it should have a low enough limit of detection (LOD) to identify infected individuals early in the disease cycle with a low rate of both false negatives (>95% sensitivity) and false positives (>95% specificity). Currently, nucleic acid amplification tests (NAATs) appear to provide the best combination of low detection limit, high sensitivity and high specificity relative to conventional binding assays such as immunoassays.[4,5]

However, the most advanced NAATs currently FDA approved, including those for POC clinical use (*i.e.*, CLIA-waived) such as those produced by Abbott, Roche, Cepheid, and Mesa Biotech, provide a complete result in ~15 minutes or more, and the typical US Medicare/Medicaid program reimbursement rate is ~\$40-50. Most NAATs rely on polymerase chain reaction (PCR) to amplify the copy number of the target, disease-specific nucleic acid (NA) in a sample and label these amplicons for subsequent detection by optical or electrochemical means. Although this approach can provide very low LODs in principle, the process is inherently complex entailing the need to isolate and purify NA from a sample so as to remove polymerase inhibitors, to control temperature cycling during the enzyme-catalyzed amplification process, to provide perishable reagents including polymerase, primers and nucleotides, and to integrate a means for labeled amplicon detection. Isothermal amplification approaches eliminate the need for temperature

cycling, but all other requirements remain. Given the process design challenges, the machines currently on the market are remarkable feats of engineering. Although one cannot rule out future advances in system design that will result in NAATs with faster turnaround times at much lower cost, many researchers have made an effort to conceive of alternate, amplification-free, NA-based pathogen detection schemes that may prove more promising.

This review focuses on discussion of published approaches for nucleic acid amplification-free detection of NA of specific sequence at the single-digit attomolar ( $\sim 1-9 \times 10^{-18}$  M) threshold or lower. The 1 aM level corresponds to  $\sim 1000$  pathogens/mL based on chromosomal NA or  $\sim 1$  viable bacterium/10 mL based on ribosomal RNA, since rRNA is present at  $\sim 10,000$  copies per viable bacterial cell. To put these numbers in perspective, the commercial, high throughput, clinical laboratory-based NAATs available for *N. gonorrhoeae* in urine have limits of detection (LODs) in the  $\sim 1 - 100$  CFU/mL range. The SARS-CoV-2 virus, the causative agent of COVID-19, is present at as low as  $10^4$  virions/mL in throat samples taken from individuals several days post initial infection.[6] Since some NAATs have practical LODs for SARS-CoV-2 of  $\geq 10^4$  copies/mL, this data may explain a significant portion of reported false negatives.[7-10] These data suggest that amplification-free methods should exhibit LODs in the low aM range or below to be competitive with NAATs and to be broadly useful for disease diagnosis. Recently, microRNAs have emerged as important disease markers and concentrations of these  $\sim 19-25$  nucleotide RNAs in blood plasma also are very low ( $< \text{pM}$ ).[11] Clearly, the technical challenges are great and this review includes mention both of approaches that may be translatable to portable, low-power POC devices as well as those technologies that may be better suited for clinical laboratory-based systems that process large batches of samples at high throughput. Although most commercialized technologies are qualitative in the sense that they give only a positive or negative



result, which is the primary objective for most disease diagnosis, most approaches described here provide the added potential benefit of being quantitative, *i.e.*, being capable of providing pathogen concentration in a sample.

## **2.2 Optical methods**

### *2.2.1 Förster resonance energy transfer (FRET)*

A common theme throughout this review is the use of nanoparticles as key components of transduction mechanisms to convert a selective hybridization event into a detectable signal. This generalization applies well to those schemes based on optical detection methods with the exception of the approach described by Ho *et al.*, which is one of the earliest reports of selective NA detection at the single-digit attomolar level or lower,[12] and is based on FRET from a cationic polythiophene to a fluorophore (Alexa Fluor 546). The FRET mechanism is exploited by combining a polymeric transducer with capture probes labeled with a fluorophore to form a duplex. Polythiophene fluorescence is quenched in this duplex state. However, once hybridized with target DNA, the cationic polymer transducer undergoes a conformational change and forms a triplex that exhibits intrinsic fluorescence at 530 nm. Energy transfer to the neighboring fluorophores bound to the ssDNA probe results in amplified emission at 572 nm upon excitation at 420 nm. Hybridization at 65 °C resulted in high stringency, and the method proved to be quantitative over the range examined. This scheme provided the lowest limit of detection (LOD) among those discussed in this review at 3 zM ( $3 \times 10^{-21}$  M) in as little as 5 min. More recently, the technique has been adapted to the microarray format for multiplex detection.[13] Analysis of more complex samples representative of those obtained in the clinic would be an important next step in development of this promising technology.

### 2.2.2 Bio-barcode method

At around the same time as the work described above, the Mirkin laboratory demonstrated a novel “bio-barcode”-based DNA detection method utilizing oligonucleotide probe-modified gold nanoparticles (AuNPs), probe-functionalized magnetic beads (MBs), and silver development for scanometric readout.[14] The AuNPs actually are conjugated with two types of oligonucleotide probes, one complementary to the target DNA and the other complementary to a barcode sequence. Since both AuNP probe and MB probe are complementary to target DNA at separate locations, a sandwich hybridization complex is formed between the AuNPs, target DNA and the MBs. This complex is separated using a magnetic field, washed, and bar-code DNA is released by heating to 55 °C. The released barcode DNA is detected by a sandwich assay using complementary oligonucleotide capture probes attached to a microscope slide and AuNPs modified with oligonucleotide probes complementary to a separate portion of the barcode DNA. Silver ions ( $\text{Ag}^+$ ) are reduced to silver metal on the AuNPs for signal amplification prior to detection based on scattered light intensity.[15] The LOD for purified anthrax DNA was estimated to be ~500 zM. Thaxton *et al.* reported an alternative to the use of heat to release barcode DNA from AuNPs based on DTT ligand exchange with thiolated barcodes.[16] Although it is not a rapid method and it involves multiple hybridization steps subject to interference, the powerful and popular barcode approach can be multiplexed and has proven broadly applicable.

### 2.2.3 Quantum dot fluorescence

Liu *et al.* appear to be the first to demonstrate the use of quantum dot (QD) fluorescence and magnetic beads (MBs) to achieve single-digit attomolar or lower detection of NAs.[17] More recently, two other groups have pursued a similar strategy.[18,19] In all cases, a sandwich assembly is created involving the MBs and QDs, and a magnetic field is used to isolate the

complexed, target DNA. The approaches differ in how QDs are used for signal amplification. Liu *et al.* use a biotinylated signal probe, streptavidin-conjugated QDs and a biotinylated linker to create a multilayer network of the fluorescent nanoparticles on the underlying sandwich assembly, and an impressive LOD of 250 zM was achieved.[17] Kim and Son use QDs with emission at 655 nm (QD<sub>655</sub>), conjugated with capture probe linked covalently to the MBs, and a signaling probe oligonucleotide, conjugated to QDs with emission at 565 nm (QD<sub>565</sub>).[18] The QD<sub>655</sub> labels serve as an internal standard to account for differences in nanoparticle concentrations among assays. Their approach proved quantitative with a LOD for ssDNA of 890 zM. Zhou *et al.* pursued a somewhat different approach using liposome-encapsulated QDs.[19] In this study, liposomes are adopted to serve as carriers encapsulating QDs of different fluorescent color for multiplexed detection. After creation of the sandwich hybridization complex and separation with the assistance of a magnetic field, the liposomes are disrupted thereby releasing hundreds of QDs to amplify the hybridization event. An LOD for HIV DNA of 1 aM was achieved with this quantitative technique and multiplexed detection of a second HIV sequence also was demonstrated. Although promising, these methods based on QD fluorescence have not yet been tested with complex clinical samples, which contain a variety of species that can interfere at multiple points in a complicated assay scheme. The need for testing with clinical samples, or at least mock clinical samples, is a common theme among early-stage technologies for amplification-free NA detection.

#### 2.2.4 Surface enhanced Raman spectroscopy (SERS) and surface plasmon resonance (SPR)

Others have pursued alternative optical techniques using AuNPs as signal enhancers enabling application of SERS and SPR for NA detection. Most recently, Liyanage *et al.* designed a scheme for label-free detection of tumor suppressor microRNAs at zeptomolar levels based on alteration of localized surface plasmon resonance when target microRNA binds to oligonucleotide

probes on triangular AuNPs (AuTNPs) (Fig. 2.1).[20] A LOD as low as 137 zM was achieved. Single base-pair mismatches also were shown to be discernable, and quantification of tumor suppressor microRNAs was demonstrated in diluted plasma samples. In earlier work, D'Agata *et al.* also used AuNP-enhanced SPR imaging to detect target human genomic DNA at 2.6 aM with selectivity for point mutations.[21] In another scheme developed by Hu *et al.*, SERS signals are enhanced both by reducing the distance between Raman labels (X-rhodamine, Rox) and AuNPs to create SERS “hot spots” enabling quantitative HIV DNA detection at the 100 zM level with selectivity toward single-base mismatches.[22] Although D'Agata *et al.* did conduct tests with blood samples,[21] all of these techniques could benefit from further validation with clinical-type samples. Nevertheless, the reliance on spectroscopy instrumentation likely will limit such approaches to the laboratory.

### 2.2.5 Darkfield microscopy

In yet another nanotechnology-based detection scheme described in this case by Li *et al.*, target DNA is sandwiched between MBs conjugated with an oligonucleotide capture probe and gold nanorods (AuNRs) conjugated with a second capture probe complementary to a separate site on the target DNA.[23] The sandwich structures are isolated from unbound AuNRs in a magnetic field and the assemblies subsequently are dehybridized at 60 °C. The recovered AuNRs, each corresponding to a single DNA target, are electrostatically bound to a positively charged glass surface modified with (3-aminopropyl)triethoxysilane. The deposited AuNRs, evident as red spots, are counted using darkfield microscopy and image recognition software. The technique was shown to be quantitative and the LOD for 63mer single-stranded DNA corresponding to the human papillomavirus (HPV) is 6.5 aM. However, lengthy hybridization steps and use of a laboratory microscope will need to be overcome, assuming detection using complex clinical samples is

demonstrated successfully. Recent demonstrations of smartphone use for optical diagnostic applications may be helpful in this regard.[24]

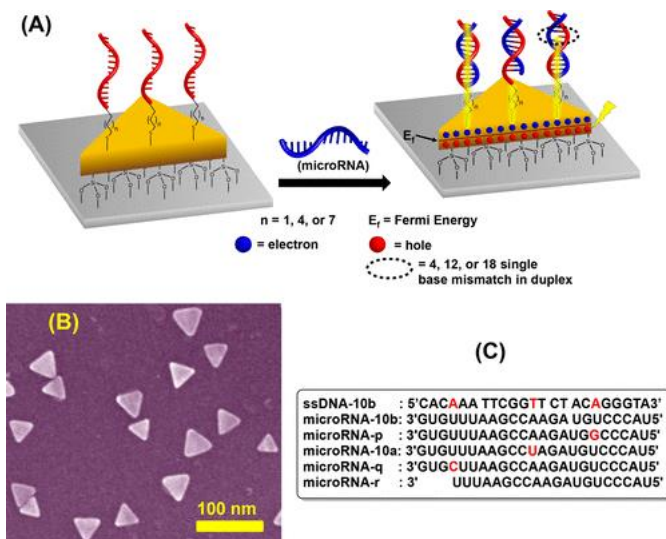


Figure 2.1. Detection of microRNA by surface plasmon resonance using triangular Au nanoparticles (see text) [20]

## 2.3 Electrochemical/Electronic methods

Electrochemical or electronic approaches for detection of NAs of specific sequence at ultralow concentration generally have been developed later than optical schemes and all within about the last 10 years, yet there is somewhat greater diversity of such technologies and a substantially greater number of corresponding publications.

### 2.3.1 Mass spectrometry (MS)

MS is based on the measurement of the mass-to-charge ratio of ions generated by ionizing a sample by various means, separating the species in an electrical or magnetic field and then detecting the separated ions. Although MS may not be widely thought of as an inexpensive medical diagnostic technique, advances in miniaturization suggest that perception may

change.[25,26] The work of Yang *et al.* serves to demonstrate one approach, based on a novel “bio-masscode” probe, where MS is used for simultaneous detection of multiple pathogen DNAs at low attomolar levels.[27] MBs and AuNPs are modified with oligonucleotide probes complementary to separate regions of the target DNAs thereby enabling hybridization to form an MB-target DNA-AuNP sandwich complex. However, the AuNPs also are modified with organic disulfide molecules that serve as the masscode for specific DNA targets. The sandwich complexes are extracted using a magnetic field, and the AuNPs are released by heating and the masscodes analyzed using matrix-assisted laser desorption ionization (MALDI), time-of-flight (TOF) MS. The technique appears to be at least semiquantitative with an LOD of ~1 aM. In a key study, hepatitis B virus DNA was detected successfully in a blood sample. However, the published protocol requires long hybridization times like many other techniques discussed in this review.

### 2.3.2 Constant potential amperometry

Perhaps the simplest electroanalytical technique is constant potential amperometry (CPA) where current is measured at a fixed potential. Spain *et al.* developed a CPA method for detection of *S. aureus* DNA based on usage of novel platinum nanoparticles (PtNPs) that have a portion of their surface area modified with an oligonucleotide capture probe and the remainder available for electrocatalyzed reduction of H<sub>2</sub>O<sub>2</sub> for signal amplification (Fig. 2.2).[28] An estimated LOD of ~1 aM was achieved and single-base pair selectivity was demonstrated. This simple technique is surprisingly powerful, however the long incubation times specified for hybridization constitute a drawback. A few years later an alternative, catalytic means to amplify a recognition event and to transduce it using CPA was demonstrated by Li *et al.*[29] Dual-thiolated, double-stranded hairpin DNA is first immobilized on the gold electrode surface as the capture probe. The biotin-labeled signal DNA is designed partially complementary to the capture loop and complementary to the

portion of the target NA that does not hybridize to the capture probe. Yet, the signal DNA itself cannot bind to the capture probe, because the melting temperature  $T_m$  of the complex is lower than the assay operation temperature of 37 °C. Once target DNA is introduced, however, signal DNA, target DNA, and capture probe can form a more extensively hybridized, Y-shaped DNA structure on the loop of the capture probe, because the  $T_m$  is higher than the working temperature. The target recognition is amplified and transduced using streptavidin-labeled horseradish peroxidase (SA-HRP), which binds to the biotin-labeled signal DNA and catalyzes the reduction of supplied  $H_2O_2$  with 3,3',5,5'-tetramethylbenzidine (TMB) serving as the electron transfer mediator with the underlying electrode. A constant reducing potential is imposed at the electrode and the steady-state current is recorded within ~100 seconds. The technique was demonstrated with PCR product DNA, mRNA and microRNA with a LOD estimated at 3 aM. This is a versatile approach that could be made more attractive if the relatively long assay time could be reduced significantly from ~1 hour.

### 2.3.3 Voltammetry

As a general class, voltametric techniques have been the most popular of electrochemical methods for detection of DNA and RNA at ultralow concentration. Of these voltametric approaches, cyclic voltammetry (CV) is the most widely known and among the most straightforward. In CV, potential at a working electrode is ramped linearly between reducing and oxidizing limits in a sawtooth wave, and the current is measured and plotted versus potential. For example, Kim *et al.* constructed a microfluidic-channel-based, electrochemical DNA biosensor that relies on CV as the detection method.[30] Gold is first plated in an electroless manner on the pore walls of anodic aluminum oxide (AAO) filtration membranes, which serve as the working electrodes. DNA oligonucleotides on the modified membrane pore surfaces serve as capture

probes. Relatively rapid hybridization in ~20 mins is achieved by flowing the target DNA solution through the modified membrane pores, and DNA was detected successfully at as low as 100 zM. This technique cleverly exploits the high surface area membrane geometry to speed hybridization and to increase assay sensitivity. The technology would appear even more promising if it were demonstrated successfully with complex clinical samples.

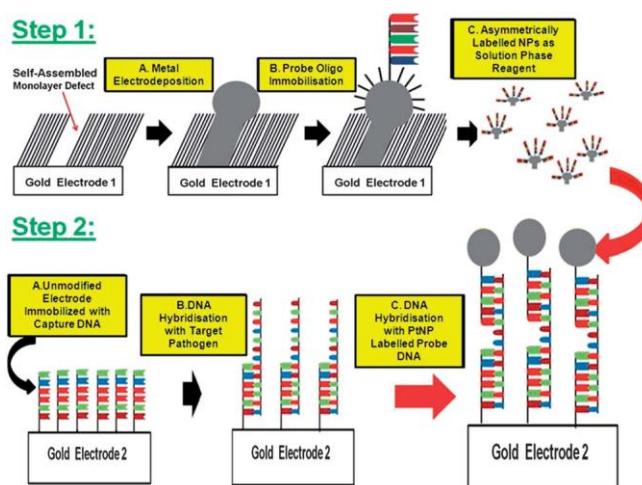


Figure 2.2. DNA detection by constant potential amperometry using Pt-labeled signal oligonucleotides and Pt-catalyzed,  $\text{H}_2\text{O}_2$  electroreduction (see text)[28]

Square wave voltammetry (SWV) is a similar technique to CV in that potential is swept between potential limits while current is monitored. However, the potential is not swept linearly as in CV, rather the potential waveform may be regarded as a square wave superimposed onto an underlying staircase change in potential. SWV provides a means to minimize the contribution of non-faradaic (i.e., charging) current to the overall signal monitored. Hu *et al.* employed electrochemically controlled reversible addition–fragmentation chain-transfer (eRAFT) polymerization in conjunction with SWV to amplify target DNA recognition events and to achieve transduction to measurable current signals.[31] The eRAFT polymerization step results in attachment of numerous electroactive ferrocenyl (Fc) tags that serve to amplify the DNA capture



events by peptide nucleic acid probes immobilized on the electrode surface. This is a promising quantitative method with a reported LOD of 4.1 aM that shows single-base selectivity and has been tested with samples containing 10% human serum, but includes specification for a lengthy 1.5-hour hybridization time.

In differential pulse voltammetry (DPV), voltage pulses are superimposed on the background potential swept linearly or in staircase mode. Like SWV, DPV isolates the faradaic component of the overall current signal thereby enabling a focus on the actual electrode reactions taking place. At least four publications have appeared describing the use of DPV to detect NAs at ultralow concentration.[32-35] In the most recent work, Widaningrum *et al.* constructed an electrochemical sensing strategy based on use of “bio-barcode” latex labels and detection of deposited Ag metal using DPV.[33] The technique is quantitative and an LOD of 560 zM was reported. Dong *et al.* also successfully constructed a scheme to detect DNA based on DPV measurements where electrochemically reduced graphene oxide (ERGO) on glassy carbon is used as the electrode material.[34] Target DNA is captured in a sandwich complex on the electrode with streptavidin–horseradish peroxidase (HRP) functionalized carbon spheres serving as signal amplifying tags. In related work, Gao *et al.* developed a sensing strategy based on the molecular beacon approach using HRP for signal amplification and measurements made using DPV.[35] Finally, Hu *et al.* developed a PNA probe-based DNA assay based on DPV measurements that entails the reduction of Ag<sup>+</sup> ions and subsequent deposition of silver metal that subsequently can be electrochemically stripped thereby offering a powerful approach that takes advantage of the DPV technique.[32] Further validation of all of these DPV-based methods using clinical-type samples is needed as well as a reduction in total assay time in most cases.

#### 2.3.4 Electrochemical impedance spectroscopy (EIS)

EIS might be considered yet another related voltametric technique where a sinusoidal (AC) potential of varied frequency is imposed at the working electrode and the resulting current signal is monitored. The corresponding, frequency-dependent impedance (potential divided by current) often is represented on a Nyquist plot. Benvidi *et al.* developed an approach based on glassy carbon electrodes modified with reduced graphene oxide (RGO).[36] DNA probes are immobilized covalently on the deposited RGO, and EIS data are gathered before and after target DNA hybridization in an aqueous solution containing  $[\text{Fe}(\text{CN})_6]^{3-/4-}$ . An increase in charge transfer resistance,  $R_{ct}$ , with target DNA concentration was observed and a remarkable LOD of 3.2 zM was achieved. Although EIS is a relatively sophisticated technique, this overall approach is straightforward and powerful. If it proves applicable to clinical samples and overall assay times could be shortened, this scheme may be among the more promising. Tripathy *et al.* developed an approach very similar to that of Benvidi *et al.* for the detection of Dengue virus DNA in whole blood in the zeptomolar range.[36,37] Finally, Sahoo *et al.* developed a label-free, EIS-dependent DNA detection method based on poly(amidoamine)dendrimer (G3-PAMAM) functionalized GaN nanowires (NWs) grown on gold.[38] A LOD of 100 zM for a synthetic H1N1 swine flu DNA sequence was achieved. As with the other EIS-based techniques, this approach appears relatively straightforward and powerful, but could be made more attractive with a reduction in overall assay time.

#### 2.3.5 Field effect transistors (FETs)

The use of field effect transistors (FETs) as sensors constitutes an entirely different approach to electrochemical NA detection. A FET is a type of transistor where the electric field at a “gate” controls the flow of current between “source” and “drain” electrodes. When configured

as a sensor, the binding of an analyte at the gate results in a change in potential that gives rise to a measurable shift in the flow of current between the source and drain. Ramnani and *et al.* demonstrated label-free and rapid detection of microRNA based on a carbon nanotube field-effect transistor (FET) functionalized with the Carnation Italian ringspot virus (CIRV) p19 protein (Fig. 3).[39] The FET device is fabricated using 3-aminopropyltriethoxysilane (APTES)-assisted assembly of carbon nanotubes (CNTs) across gold electrodes acting as source and drain. The CNTs are subsequently modified with CIRV p19. The microRNA target, miRNA-122a, which is a specific liver marker, is first hybridized to a complementary RNA probe to form a double-stranded complex. This complex subsequently is contacted with CIRV p19 on the FET sensor surface. CIRV p19 shows high and selective affinity only for shorter, double stranded/duplex RNA, but not to tRNA, rRNA or DNA. The binding of the miRNA-RNA probe complex to p19 results in a change of conductance of the CNTs, which is quantified by measuring the change in resistance evident from the FET I-V curve. The LOD was estimated at ~1 aM against a large background of nontarget RNA and quantitative detection in the range of 1 aM to 10 fM also was demonstrated. Although the total assay time is over 2 hours, this method is attractive for challenging, quantitative microRNA detection. Notably, Chen *et al.* introduced the concept of a GaN nanowire (GaNNW) based extended-gate FET (EGFET) biosensor for ultralow NA detection where the GaNNWs are exposed to the sample solution and are connected to a commercial metal-oxide semiconductor FET (MOSFET) via a metal wire.[40] A similar LOD was estimated at ~1 aM, yet a shorter, more encouraging assay time of ~30 minutes was demonstrated.

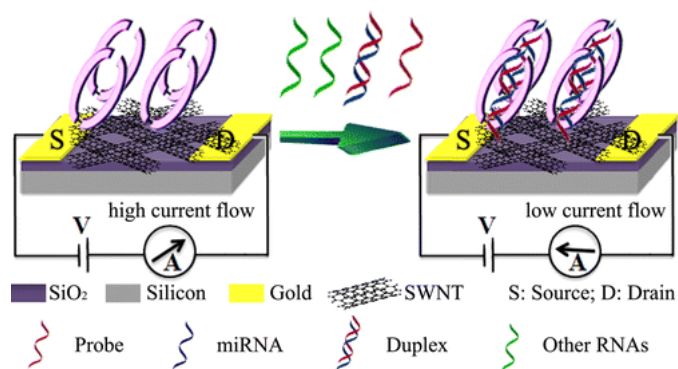


Figure 2.3. microRNA detection using carbon nanotube field effect transistors functionalized with the Carnation Italian ringspot virus p19 protein (see text)[39]

### 2.3.6 Piezoelectric plate sensor

In yet another approach demonstrating the diversity of electrochemical approaches, a 1.6 aM DNA LOD was achieved using a piezoelectric plate sensor consisting of an 8- $\mu\text{m}$ -thick lead magnesium niobate-lead nitrate (PMN-PT) cantilever layer sandwiched between Cr/Au electrodes and insulated with 3-mercaptopropylmethoxysilane.[41] Wu *et al.* immobilized a oligonucleotide probe for hepatitis B viral DNA on the cantilever surface and monitored the shift in length extension or width extension mode resonance peak frequency upon 200mer target HBV DNA binding in buffer solution.[41] A sensor response is evident in less than 10 mins, however it is unclear how well the sensor will work with target in complex sample media.

## 2.4 Nanopore sensors

Most nanopore-based NA sensing systems are based on a resistive-pulse sensing mechanism following on the work of Coulter,[42] where the conductance of an electrolyte-filled pore or channel is monitored as analyte species traverse it. Rahman *et al.* pursued this general strategy while also taking advantage of optical trapping to enhance counting of target DNA species using nanopores.[43] The LOD was estimated at  $\sim 1$  aM, and the DNA counting process is

accomplished in just a few minutes, which is remarkable. However, the study appears to have been conducted with purified DNA and requires electronics capable of resolving millisecond-timescale, nA deflections in current. Rather than measure small, short-lived deflections in current as target species traverse a small diameter nanopore, the detection technique described by Koo *et al.* entails simple conductometric detection of much-larger-pore blockage events.[44] The method relies on an electromechanical signal transduction mechanism that also enables detection of NA at ~1 aM. Uncharged PNA capture probes are conjugated to ~800-nm-diameter polystyrene spheres that are designed to be very nearly charge neutral overall such that they do not exhibit electrophoretic movement in the presence of an electric field. However, the substantial negative charge acquired upon capture of a target NA sequence makes the hybridized conjugate mobile. Electrophoresis of the bead-PNA conjugate with hybridized target NA to the mouth of a smaller diameter glass pore causes a significant decrease in pore conductance, thereby resulting in a strong, sustained drop in measured ionic current. Nonspecifically bound NA is removed from the bead conjugate by the strong electric field at the pore mouth resulting in no sustained signal. Further, the opposing electroosmotic flow through the glass pore sweeps PNA-bead conjugates without hybridized target away from the pore mouth. In such a way, this simple conductometric device gives a highly selective (no observed false positives), binary response signaling the presence or absence of the target NA. *E. coli* rRNA was detected at 1 aM against a large background of *P. putida* RNA. With a substantial decrease in overall assay time, this simple, potentially inexpensive, label-free technique may hold promise.

## **2.5 Conclusion and outlook**

The COVID-19 pandemic has brought the need back into focus for rapid, user-friendly, inexpensive, sensitive and accurate disease diagnostics. Commercially available nucleic acid (NA)

amplification tests (NAATs) serve as the standard for both point-of-care (POC) and clinical laboratory-based disease diagnostics, yet the current assay time of ~15 minutes or more for the POC technology and the cost of these assays makes them nonideal. Mostly within the past 10 years, there has been a steady stream of reports describing NA amplification-free methods applicable to detection of pathogen-specific DNA or RNA at the most clinically desirable LODs of single-digit attomolar or lower. Such approaches hold promise for the development of faster, less expensive diagnostic systems. With the added urgency made evident by the pandemic, the appearance of publications reporting amplification-free techniques is expected to accelerate, which makes this review timely. Without question, the emergence of nanotechnology has enabled conception of nearly all of the novel approaches with ultralow LODs published, which incorporate nanoparticles, fluorescent quantum dots, nanorods, nanowires and nanotubes. The broad spectrum of possible schemes also builds upon the very diverse arsenal of optical and electrical measurement devices available. However, very few of the methods described in this review have been tested sufficiently with clinical, or even mock clinical samples, that typically contain many species capable of interfering with an assay; and even fewer of the detection technologies have been integrated into complete diagnostic devices for which an overall assay time can be established. Lengthy reported hybridization times alone for many of these amplification-free schemes exceed the overall assay time for commercial NAATs. There are published means to reduce hybridization steps to just a few minutes,[45] but such selective binding events are possible points of error and interference by the myriad species present in actual clinical samples. It should be expected that methods reliant on the fewest reagents and selective binding events as well as the simplest electrical or optical measurements such as constant potential amperometry, conductimetry, light scattering, and fluorescence might have the greatest potential for eventual commercial success.

Also, a number of developments have emerged in the recent literature that may eventually lead to additional schemes for ultralow, amplification-free NA detection including CRISPR technology.[46,47] Based on the available evidence, it appears likely that during the next several years some new and exciting NA-based disease diagnostic technology will emerge commercially.

## 2.6 References

1. Atkinson LM, Vijeratnam D, Mani R, Patel R, '*The waiting game*': are current *chlamydia and gonorrhoea near-patient/point-of-care tests acceptable to service users and will they impact on treatment?* Int J STD AIDS, 2016. **27**: p. 650-655.
2. Hsieh YH, Hogan MT, Barnes M, Jett-Goheen M, Huppert J, Rompalo AM, Gaydos CA, *Perceptions of an ideal point-of-care test for sexually transmitted infections--a qualitative study of focus group discussions with medical providers.* PLoS One, 2010. **5**:e14144.
3. Jayamohan H, Sant HJ, Gale BK, *Applications of microfluidics for molecular diagnostics.* Methods Mol. Biol (N. Y., NY, U. S.), 2013. **949**: p.305-334.
4. Cristillo AD, Bristow CC, Peeling R, Van Der Pol B, de Cortina SH, Dimov IK, Pai NP, Shin DJ, Chiu RYT, Klapperich C, et al., *Point-of-Care Sexually Transmitted Infection Diagnostics: Proceedings of the STAR Sexually Transmitted Infection-Clinical Trial Group Programmatic Meeting.* Sexually Transmitted Diseases, 2017. **44**: p. 211-218.
5. Lui C, Cady NC, Batt CA, *Nucleic Acid-based Detection of Bacterial Pathogens Using Integrated Microfluidic Platform Systems.* Sensors (Basel), 2009. **9**: p. 3713-3744.
6. Pan Y, Zhang D, Yang P, Poon LLM, Wang Q, *Viral load of SARS-CoV-2 in clinical samples.* The Lancet Infectious Diseases, 2020. **20**: p. 411-412.

7. Metsky HC, Freije CA, Kosoko-Thoroddsen T-SF, Sabeti PC, Myhrvold C, *CRISPR-based surveillance for COVID-19 using genomically-comprehensive machine learning design*. bioRxiv, 2020. p.1-11.
8. Wang M, Fu A, Hu B, Tong Y, Liu R, Gu J, Liu J, Jiang W, Shen G, Zhao W, et al., *Nanopore target sequencing for accurate and comprehensive detection of SARS-CoV-2 and other respiratory viruses*. medRxiv, 2020. p. 1-29.
9. Jung YJ, Park G-S, Moon JH, Ku K, Beak S-H, Kim S, Park EC, Park D, Lee J-H, Byeon CW, et al., *Comparative analysis of primer-probe sets for the laboratory confirmation of SARS-CoV-2*. bioRxiv, 2020. p. 1-13.
10. Lucia C, Federico P-B, Alejandra GC, *An ultrasensitive, rapid, and portable coronavirus SARS-CoV-2 sequence detection method based on CRISPR-Cas12*. bioRxiv, 2020. p. 1-10.
11. Jet T, Gines G, Rondelez Y, Taly V, *Advances in multiplexed techniques for the detection and quantification of microRNAs*. Chemical Society Reviews, 2021.
12. Ho HA, Dore K, Boissinot M, Bergeron MG, Tanguay RM, Boudreau D, Leclerc M, *Direct molecular detection of nucleic acids by fluorescence signal amplification*. Journal of the American Chemical Society, 2005. **127**: p. 12673-12676.
13. Najari A, Ho HA, Gravel J-F, Nobert P, Boudreau D, Leclerc M, **Reagentless** *Ultrasensitive Specific DNA Array Detection Based on Responsive Polymeric Biochips*. Analytical Chemistry, 2006. **78**: p. 7896-7899.
14. Nam JM, Stoeva SI, Mirkin CA, *Bio-bar-code-based DNA detection with PCR-like sensitivity*. Journal of the American Chemical Society, 2004. **126**: p. 5932-5933.



15. Taton TA, Mirkin CA, Letsinger RL, *Scanometric DNA Array Detection with Nanoparticle Probes*. Science, 2000. **289**: p. 1757.
16. Thaxton CS, Hill HD, Georganopoulou DG, Stoeva SI, Mirkin CA, A bio-bar-code assay based upon dithiothreitol-induced oligonucleotide release. Analytical Chemistry, 2005. **77**: p. 8174-8178.
17. Liu YJ, Yao DJ, Chang HY, Liu CM, Chen C, *Magnetic bead-based DNA detection with multi-layers quantum dots labeling for rapid detection of Escherichia coli O157:H7*. Biosensors & Bioelectronics, 2008. **24**: p. 558-565.
18. Kim GY, Son A, *Development and characterization of a magnetic bead-quantum dot nanoparticles based assay capable of Escherichia coli O157:H7 quantification*. Anal Chim Acta. 2010. **677**: p. 90-96.
19. Zhou J, Wang QX, Zhang CY, Liposome-quantum dot complexes enable multiplexed detection of attomolar DNAs without target amplification. J Am Chem Soc, 2013. **135**: p. 2056-2059.
20. Liyanage T, Masterson AN, Oyem HH, Kaimakliotis H, Nguyen H, Sardar R, *Plasmoelectronic-Based Ultrasensitive Assay of Tumor Suppressor microRNAs Directly in Patient Plasma: Design of Highly Specific Early Cancer Diagnostic Technology*. Anal Chem, 2019. **91**: p. 1894-1903.
21. D'Agata R, Breveglieri G, Zanolini LM, Borgatti M, Spoto G, Gambari R, *Direct detection of point mutations in nonamplified human genomic DNA*. Anal Chem, 2011. **83**: p. 8711-8717.

22. Hu J, Zheng PC, Jiang JH, Shen GL, Yu RQ, Liu GK, *Sub-attomolar HIV-1 DNA detection using surface-enhanced Raman spectroscopy*. *Analyst*, 2010. **135**: p. 1084-1089.
23. Li G, Zhu L, Wu Z, He Y, Tan H, Sun S, *Digital Concentration Readout of DNA by Absolute Quantification of Optically Countable Gold Nanorods*. *Anal Chem*, 2016. **88**: p. 10994-11000.
24. Contreras-Naranjo JC, Wei Q, Ozcan A, *Mobile Phone-Based Microscopy, Sensing, and Diagnostics*. *IEEE Journal of Selected Topics in Quantum Electronics*, 2016. **22**: p. 1-14.
25. Ma X, Ouyang Z, *Ambient ionization and miniature mass spectrometry system for chemical and biological analysis*. *Trends Analyt Chem*. 2016. **85**: p. 10-19.
26. Zhang W, Wang X, Xia Y, Ouyang Z, *Ambient Ionization and Miniature Mass Spectrometry Systems for Disease Diagnosis and Therapeutic Monitoring*. *Theranostics*, 2017. **7**: p. 2968-2981.
27. Yang B, Gu K, Sun X, Huang H, Ding Y, Wang F, Zhou G, Huang LL, *Simultaneous detection of attomolar pathogen DNAs by Bio-MassCode mass spectrometry*. *Chem Commun (Camb)*, 2010. **46**: p. 8288-8290.
28. Spain E, McArdle H, Keyes TE, Forster RJ, *Detection of sub-femtomolar DNA based on double potential electrodeposition of electrocatalytic platinum nanoparticles*. *Analyst*, 2013. **138**: p. 4340-4344.
29. Li C, Wu D, Hu X, Xiang Y, Shu Y, Li G, *One-Step Modification of Electrode Surface for Ultrasensitive and Highly Selective Detection of Nucleic Acids with Practical Applications*. *Anal Chem*, 2016. **88**: p. 7583-7590.

30. Kim YJ, Jones JE, Li H, Yampara-Iquise H, Zheng G, Carson CA, Cooperstock M, Sherman M, Yu Q, *Three-dimensional (3-D) microfluidic-channel-based DNA biosensor for ultra-sensitive electrochemical detection*. Journal of Electroanalytical Chemistry, 2013. **702**: p. 72-78.
31. Hu Q, Kong J, Han D, Niu L, Zhang X, *Electrochemical DNA Biosensing via Electrochemically Controlled Reversible Addition-Fragmentation Chain Transfer Polymerization*. ACS Sens, 2019. **4**: p. 235-241.
32. Hu Q, Hu W, Kong J, Zhang X, *PNA-based DNA assay with attomolar detection limit based on polygalacturonic acid mediated in-situ deposition of metallic silver on a gold electrode*. Microchimica Acta, 2014. **182**: p. 427-434.
33. Widaningrum T, Widyastuti E, Pratiwi FW, Faidoh Fatimah AI, Rijiravanich P, Somasundrum M, Surareungchai W, *Sub-attomolar electrochemical measurement of DNA hybridization based on the detection of high coverage biobarcode latex labels at PNA-modified screen printed electrodes*. Talanta, 2017. **167**: p. 14-20.
34. Dong H, Zhu Z, Ju H, Yan F, *Triplex signal amplification for electrochemical DNA biosensing by coupling probe-gold nanoparticles-graphene modified electrode with enzyme functionalized carbon sphere as tracer*. Biosens Bioelectron, 2012. **33**: p. 228-232.
35. Gao W, Dong H, Lei J, Ji H, Ju H, *Signal amplification of streptavidin-horseradish peroxidase functionalized carbon nanotubes for amperometric detection of attomolar DNA*. Chem Commun (Camb), 2011. **47**: p. 5220-5222.

36. Benvidi A, Rajabzadeh N, Mazloun-Ardakani M, Heidari MM, Mulchandani A, *Simple and label-free electrochemical impedance Amelogenin gene hybridization biosensing based on reduced graphene oxide*, Biosens Bioelectron, 2014. **58**: p.145-152.
37. Tripathy S, Krishna Vanjari SR, Singh V, Swaminathan S, Singh SG, *Electrospun manganese (III) oxide nanofiber based electrochemical DNA-nanobiosensor for zeptomolar detection of dengue consensus primer*. Biosens Bioelectron, 2017. **90**: p. 378-387.
38. Sahoo P, Suresh S, Dhara S, Saini G, Rangarajan S, Tyagi AK, *Direct label free ultrasensitive impedimetric DNA biosensor using dendrimer functionalized GaN nanowires*. Biosens Bioelectron, 2013. **44**: p. 164-170.
39. Ramnani P, Gao Y, Ozsoz M, Mulchandani A, *Electronic detection of microRNA at attomolar level with high specificity*. Anal Chem, 2013. **85**: p. 8061-8064.
40. Chen CP, Ganguly A, Lu CY, Chen TY, Kuo CC, Chen RS, Tu WH, Fischer WB, Chen KH, Chen LC, *Ultrasensitive in situ label-free DNA detection using a GaN nanowire-based extended-gate field-effect-transistor sensor*. Anal Chem, 2011. **83**: p. 1938-1943.
41. Wu W, Kirimli CE, Shih WH, Shih WY, *Real-time, in situ DNA hybridization detection with attomolar sensitivity without amplification using  $(pb(Mg_{1/3}Nb_{2/3})O_3)_{0.65}-(PbTiO_3)_{0.35}$  piezoelectric plate sensors*. Biosens Bioelectron, 2013. **43**: p. 391-399.
42. DeBlois RW, Bean CP, *Counting and Sizing of Submicron Particles by the Resistive Pulse Technique*. Review of Scientific Instruments, 1970. **41**: p. 909-916.
43. Rahman M, Harrington M, Stott MA, Li Y, Sampad MJN, Yuzvinsky TD, Hawkins AR, Schmidt H, *Optical trapping assisted detection rate enhancement of single molecules on a nanopore optofluidic chip*. Optica, 2019. **6**.

44. Koo B, Yorita AM, Schmidt JJ, Monbouquette HG, *Amplification-free, sequence-specific 16S rRNA detection at 1 aM*. Lab Chip, 2018. **18**: p. 2291-2299.
45. Henry OYF, O'Sullivan CK, Rapid DNA hybridization in microfluidics. Trac-Trends in Analytical Chemistry, 2012. **33**: p. 9-22.
46. Gootenberg JS, Abudayyeh OO, Kellner MJ, Joung J, Collins JJ, Zhang F, *Multiplexed and portable nucleic acid detection platform with Cas13, Cas12a, and Csm6*. Science, 2018. **360**: p. 439.
47. Myhrvold C, Freije CA, Gootenberg JS, Abudayyeh OO, Metsky HC, Durbin AF, Kellner MJ, Tan AL, Paul LM, Parham LA, et al., Field-deployable viral diagnostics using CRISPR-Cas13. Science, 2018. **360**: p. 444.

### **Chapter 3: Simplified NA extraction and enhanced kinetic hybridization for amplification-free, sequence-specific 16S rRNA detection at 100 zM**

#### **Abstract**

An amplification-free, nanopore-based nucleic acid detection method with simplified nucleic acid extraction and kinetically enhanced hybridization has been demonstrated for rapid, rRNA sequence-specific detection of *Escherichia coli* (*E. coli*) at the ultralow concentration of 100 zM ( $10^{-19}$  M). This work was motivated by the need for simple, rapid, and low-cost detection of species-specific bacterial infection at low concentration. In our system, an amine-terminated peptide nucleic acid (*i.e.*, an uncharged polyamide analog to DNA/RNA) probe complementary to *E. coli* 16S rRNA, is covalently bound to carboxyl-functionalized polystyrene microbeads to form a charge neutral bead-probe conjugate. After exposure to the sample, the target 16S rRNA hybridizes with the complementary PNA probe conjugated to the microbeads. Driven by an externally applied electric field, the PNA-microbeads with negative charge added by hybridized rRNA are driven to a smaller diameter nanopore on a glass chip and at least partially block it resulting in a sustained drop in ionic current thereby signaling the presence of the target rRNA. Simplified nucleic acid extraction was accomplished using 0.1 M NaOH followed by simple filtration with 0.02  $\mu\text{m}$  pore diameter membrane. Kinetically enhanced hybridization was achieved by flowing RNA-containing samples through a compact bed of PNA beads, which assured better interfacial contact between the PNA-beads and target RNA. Alkaline extraction and this kinetically enhanced hybridization enabled us to accomplish lab-based sample pretreatment within 30 minutes. The longest detection time took about 25 minutes, which occurred at the lowest concentration of 16S rRNA (100 zM). These results suggest that this technology with improved sample

pretreatment have great potential for developing a rapid, inexpensive, low-cost pathogen detection system for point-of-care applications.

### **3.1 Introduction**

The ongoing COVID-19 pandemic has last for over two years, and has caused millions of deaths. This worldwide, public crisis has made the need for rapid, sensitive, and inexpensive point-of-care (POC) disease diagnostics readily apparent. An ideal POC diagnostic system should be rapid and reliable so that patients can be treated optimally without the need for undependable follow up visits to the clinic. It also should be inexpensive so that it is affordable for most of the patient population. Lastly, the diagnostic system should be easy for people without complicated training to operate, the ideal case would require only loading sample and pressing a button.[1] Currently, most existing clinical sample analyses with high sensitivity and specificity, and low LOD are conducted using lab-based nucleic acid amplification tests (NAATs) with turnaround times of one day or more. [2, 3] However, NA amplification relies on systems for precise reaction control and expensive reagents such as primers, polymerase, and nucleotides.

Over the past 10 years, many remarkable studies have been reported with NA amplification-free systems with low LODs and high sensitivity. Optical methods are common themes that utilize nanoparticles, such as gold nanoparticles, functionalized magnetic beads and quantum dot fluorescence, as the key elements to convert a selective hybridization event into an optical signal.[4-10] Yet the requirement for optical components increases complexity and cost. Electrochemical approaches provide ultralow concentration detection by transducing chemical signals into electric signals. Constant potential amperometry (CPA) is a simple electroanalytical technique that measure cell current at fixed potential, and it can be used to achieve LODs in the single-digit attomolar range. [11, 12] Voltammetry (CV) is another technique for NA detection at

ultralow concentration by measuring the current versus potential of a characteristic redox process. [13, 14] Field effect transistors (FETs) embody yet a different approach that utilize an electric field as a “gate” to control the flow of current between “source” and “drain”. Target NA binding results in a change in potential at the “gate”, which causes a current shift between the “source” and “drain” thereby providing the detection signal. Such FET sensors can also achieve a LOD in the single-digit attomolar range. [15, 16] Yet the need for expensive labels and/or lengthy assay times have been drawbacks of these otherwise promising electrochemical approaches.

Nanopore technology has also been used to sense NA based on the resistive-pulse sensing (RPS) mechanism, which analyzes the conductance through the electrolyte-filled pore as analyte species pass through it [17]. With the advantage of optical trapping technics, nanopore RPS sensing has achieved a LOD of  $\sim 1$  aM. [18] In contrast, our group developed a nanopore sensor to detect sequence-specific 16S rRNA of bacterial pathogens based on pore blockage. [19] Since each viable bacterial cell contains  $\geq 10,000$  copies of rRNA, better sensitivity could be achieved by detecting rRNA compared to tests based on low copy number DNA.[20] In our system, peptide nucleic acid (PNA), an uncharged polyamide analog to DNA/RNA, is covalently bound to carboxyl-functionalized polystyrene microbeads to form charge neutral bead-probe conjugates. When the neutral PNA-microbeads hybridize with target rRNA, they gain substantial negative charge and therefore exhibit mobility in an electric field. If the complex is directed to a smaller diameter pore in a glass membrane, it will at least partially block it, resulting in a sustained drop in ionic current thereby signaling the presence of the target rRNA. In prior work, the extraction of 16S rRNA, and hybridization between the bead-PNA conjugates and target 16S rRNA took 2 hours and 8 hours, respectively. In addition, the previously reported LOD for this system is about 1 attomolar (aM,  $10^{-18}$ ) but with a long detection time of 40 minutes. Therefore, the overall assay



time must be reduced to make the technology more applicable at the POC. In this study, we focused on reducing the total detection time by simplifying both RNA extraction and hybridization.

## 3.2 Materials and methods

### 3.2.1 Reagents

Carboxyl-functionalized, 820 nm-dia. polystyrene microspheres and 0.02  $\mu\text{m}$  pore dia. Vivaspin® 2 mL ultrafiltration devices were purchased from Bangs Laboratories, Inc. (Fishers, IN). 1-Ethyl-3-(3-dimethylaminopropyl)carbodiimide hydrochloride (EDC) was obtained from ThermoFisher Scientific (Waltham, MA). 2-(*N*-Morpholino)ethanesulfonic acid (MES), methoxypolyethylene glycol amine (mPEG-amine) and ethanolamine were purchased from Sigma-Aldrich (St. Louis, MO). Peptide nucleic acid (PNA) probes were synthesized by PNA Bio (Thousand Oaks, CA) and arrived as >95% HPLC-purified, lyophilized powders. The target PNA probe sequence for detecting *E. coli* 16S rRNA was  $\text{NH}_2\text{-(CH}_2\text{CH}_2\text{OCH}_2\text{CH}_2\text{OCH}_2\text{CO)}_6\text{-CTCCTTCCC TCA TTT CA}$ . [21] *E. coli* (ATCC 25922), *P. putida* (ATCC 12633), ATCC Medium 18: trypticase soy broth and ATCC Medium 3: nutrient broth were purchased from American Type Culture Collection (Manassas, VA). RNeasy protect bacteria mini kit was purchased from Qiagen (Redwood City, CA). Two mm-diameter, 4 mm-long Ag/AgCl pellet electrodes were secured from A-M systems, Inc. (Carlsborg, WA). GE Healthcare Life Sciences Anotop 25 syringe filters (25 mm-diameter, 0.02  $\mu\text{m}$  pore) were supplied by Genesee Scientific (San Diego, CA).

### 3.2.2 Coupling PNA probe to microspheres

To prepare microspheres to be conjugated with PNA, one  $\mu\text{L}$  of 820 nm-dia. carboxyl-functionalized polystyrene microspheres, at a stock concentration of  $3.25 \times 10^{11}/\text{mL}$  were suspended in 500  $\mu\text{L}$  MES buffer, pH 4.5. The beads were washed 3 times by centrifugation at

14,000 rpm for 15 minute and resuspension in fresh MES buffer. After the third wash, the beads were resuspended in 600  $\mu$ L MES buffer, and EDC (200 mM final concentration) was added to the suspension to serve as a crosslinker between the carboxyl groups on the polystyrene microbeads and the terminal primary amine groups on the PNA probes. The bead and EDC preparation was incubated for 15 minutes at 50 °C. Next, 1.14 nmol of the PNA probe was added followed by incubation for 2 hours at 50 °C. Subsequently, mPEG-amine was added to a final concentration of 100 mM, and the mixture was incubated for another 1 hour at 50 °C. This latter conjugation step was designed to reduce bead aggregation. Finally, ethanolamine was added to final concentration of 138 mM and incubated for yet another hour at 50 °C. Ethanolamine served to cap remaining carboxylic groups, thereby ensuring that the PNA conjugated beads were nearly charge neutral. After the surface modification of the polystyrene microbeads, they were washed 3 times with 0.4 $\times$  SSC (60 mM NaCl, 6 mM trisodium citrate, 0.1% Triton X-100, pH 8). Each wash consisted of centrifugation at 14,000 rpm for 15 mins, followed by resuspension in 0.4 $\times$  SSC. One fourth of the final bead preparation was taken for zeta potential measurement, and the remainder was resuspended and stored in hybridization buffer (10 mM NaCl, 25 mM Tris-HCL, pH 7). The zeta potential of the PNA-beads was measured in testing buffer (10 mM KCl, 5.5 mM HEPES, 0.01% Tween-80, pH 7) with a Malvern Zetasizer Nano ZS (Malvern Instruments Ltd, Worcestershire, England). A zeta potential in the negative single-digit mV range was taken as evidence of successful microbead surface modification.

### 3.2.3 Cell culturing

Cultures of *E. coli* and *P. putida* were initiated by suspension of the lyophilized preparations in soy (ATCC Medium 18) and nutrient (ATCC Medium 3) media, respectively, followed by incubation. *E. coli* subsequently was cultured in shake flasks at 37 °C and 250 rpm,

and *P. putida* at room temperature and 250 rpm. The initial culture was divided into aliquots which were stored at -80 °C to serve later as inocula. To prepare culture for RNA extraction, a small portion of frozen *E. coli* and *P. putida* were mixed into 3mL of soy and nutrient media, respectively. Culturing conditions were same as described above. Both bacterial was grown to log phase with approximately OD of ~0.5.

#### 3.2.4 RNA extraction

RNeasy protect bacteria mini kit from Qiagen was used to extract high purity RNA. To start the extraction, 1.7 mL of bacterial culture was pelleted out followed by 45 minutes of enzymatic lysis. The cell lysate was transferred into RNeasy spin column for purification and the final RNA was eluted into 100 µL of RNase-free purified water.

Lysis under alkaline conditions followed by simple filtration was performed as a more efficient method suitable for our detection scheme.[22] This latter approach entailed centrifugation of 1 mL of culture at 14,000 rpm for five minutes followed by resuspension of the cell pellet in 200 µL of 0.1 M NaOH (pH 13.2) for bacterial lysis. After incubation for 1 minute, 400 µL of 0.2 M Tris-HCl (pH 4.5) was added to neutralize the preparation. Immediately after, a 0.02-µm syringe filter was used to remove cell debris. The concentration and purity of the total RNA were measured using a Thermo Scientific Nanodrop 2000. From the previous study regarding the percentage of 16S rRNA in total RNA for *E. coli* and *P. putida*, the concentration of 16S rRNA in the samples of extracted RNA from *E. coli* and *P. putida* were estimated and are reported in Table 3.1.[23]

### 3.2.5 Hybridization of RNA to PNA-bead conjugate

According to our previous work, a specific volume of extracted RNA was added to approximate  $1.26 \times 10^6$  PNA-bead conjugates in 600  $\mu\text{L}$  hybridization buffer to give the desired approximate 16S rRNA concentration. Hybridization was permitted to occur at room temperature for 8 hours on a rotator. PNA-beads with hybridized target were then cleaned with Vivaspin® 2 mL ultrafiltration devices using centrifugation at 700 rpm for five minutes. The final product was suspended in 200  $\mu\text{L}$  of testing buffer. [19]

Kinetically enhanced hybridization was achieved in 2 mL, 0.02  $\mu\text{m}$  pore dia. Vivaspin® ultrafiltration devices. As shown in Figure 3.1, PNA beads in hybridization buffer first were transferred to the Vivaspin® devices and centrifuged at 1000 rpm for 5 minutes to sediment the bead-PNA conjugates in ~2-layer deep bed on the porous membrane. The RNA preparation of known concentration then was added to the same Vivaspin® device and spun at 1000 rpm for 5 minutes to facilitate intimate contact of the extracted RNA with the deposited bead-PNA resulting in hybridization of target 16S rRNA. After washing with 0.4 $\times$  SSC buffer, hybridized beads were collected in testing buffer by the reverse spinning of the Vivaspin® device.

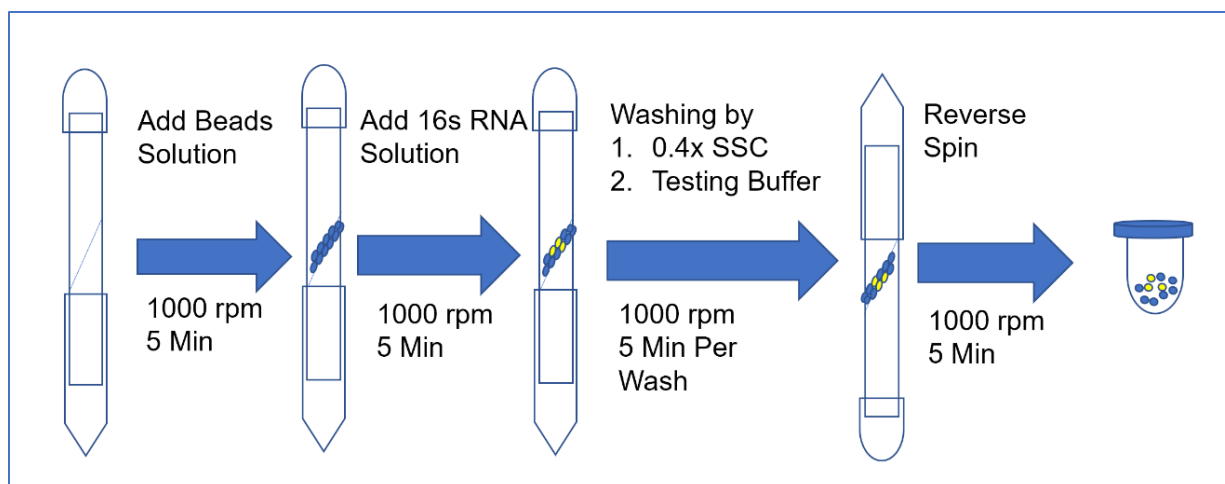
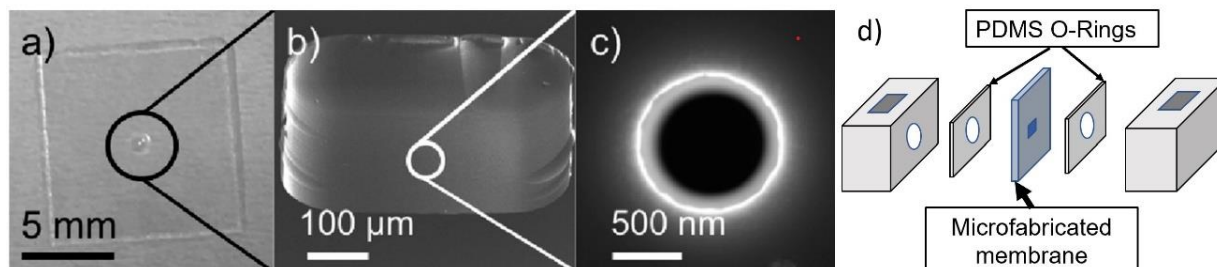


Figure 3.1. Schematic of kinetic enhanced hybridization between PNA beads and the target RNA

### 3.2.6 Sample detection

According to earlier work, 4-in. borosilicate glass wafers (Plan Optik, Elsoff, Germany) was used to microfabricate the glass chip with nanopore. A  $\sim 0.25 \text{ mm}^2$ ,  $1 \text{ }\mu\text{m}$ -thick membrane was firstly wet etched in the center of the chip with hydrofluoric acid (89% water, 10% hydrofluoric acid and 1% hydrochloric acid). A  $\sim 500 \text{ nm}$  pore was then bored in the center of the membrane with a focused ion beam (FEI Nova 600 Nanolab DualBeam SEM/FIB).[19] The glass chip was sandwiched by two Teflon chambers ( $6 \text{ mm} \times 6 \text{ mm} \times 8 \text{ mm}$ ) using polydimethylsiloxane (PDMS) O-rings as seals (Figure 3.2). Each chamber was filled with  $200 \text{ }\mu\text{L}$  of testing buffer. A Ag/AgCl pellet electrode was placed in each chamber, and both electrodes were connected to a multichannel potentiostat (VMP3). EC-Lab software (Bio-Logic USA, LLC, Knoxville, TN) was used to control the voltage across the nanopore and record the ionic current over time. Hybridized PNA-bead samples were injected into the chamber with liquid contacting the smooth backside (opposite to the etched well) of the glass chip. After the addition of the sample, a voltage of  $1.5 \text{ V}$  was applied across the nanopore and the current over time was recorded. After each detection signal, indicated by 60 seconds of sustained ionic current drop, the polarity

of the electronic field was reversed to  $-1.5\text{ V}$  to attempt to unblock the pore. After  $\sim 1$  min of reversed polarity, the field was flipped back to  $1.5\text{ V}$  to confirm baseline current recovery and detection signal reproducibility.



**Figure 3.2** Glass chip and detector assembly. a) The  $1\text{ cm} \times 1\text{ cm}$  chip with  $\sim 1\text{ }\mu\text{m}$ -thick membrane and pore in the center. b) Micrograph of the  $\sim 1\text{ }\mu\text{m}$ -thick membrane at the chip center. c) Micrograph of the  $\sim 500\text{ nm}$  pore at the center of the glass membrane. d) The glass chip sandwiched between Teflon chambers ( $6\text{ mm} \times 6\text{ mm} \times 8\text{ mm}$ ).

### 3.3 Results and discussion

In previous work, we demonstrated detection of *E. coli* 16S rRNA at  $\sim 1\text{ aM}$  against a background of  $\sim 1\text{ pM}$  of *P. putida* RNA. In this study, an attempt was made to push the limit of detection (LOD) lower while also exploring more rapid methods to extract RNA and to hybridize target rRNA with complementary PNA probe conjugated to polystyrene beads. Results illustrated in Figure 3.3 show clear, sustained drops in ionic current at  $\sim 100\text{ zM}$  *E. coli* 16S rRNA prepared using the Qiagen kit and after hybridization overnight. Note that the voltage polarity was reversed briefly after the first and second step changes in current to drive PNA-beads with hybridized target rRNA away from the glass pore in order to confirm detection when the operating voltage was re-applied. No detection signals were observed at  $10\text{ zM}$  *E. coli* 16S rRNA, which suggests that the LOD of our nanopore system is in the  $\sim 100\text{ zM}$  range. One interesting point is that the first detection event onset time varied from  $\sim 600$  seconds to  $\sim 2500$  seconds among the tests with  $100\text{ zM}$  RNA. By hybridizing PNA beads with  $600\text{ }\mu\text{L}$  RNA sample at the concentration of  $100\text{ zM}$ , less than

forty PNA-beads with bound target rRNA would be expected in the preparation, and therefore the dispersed initial position of injected beads could account for the variation of detection time. Since the greatest electric field existed near the pore mouth, the target bead conjugates would first diffuse from the chamber to the nanopore proximity. If the target bead conjugates located far away from the nanopore, the extra diffusion time would be added to the total detection time.

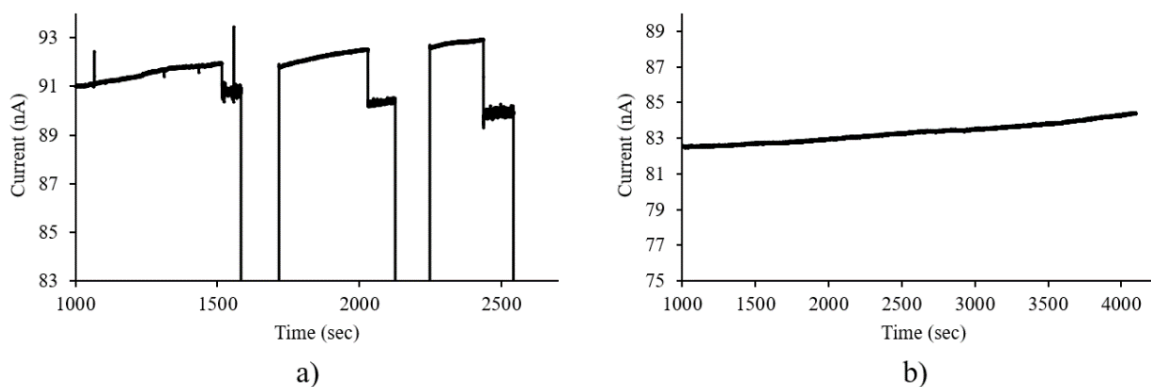


**Figure 3.3.** PNA-beads tests with Qiagen extraction kit and over-night hybridization. a) shows repeated, consistent current drops using in a concentration of 100 zM *E. coli* 16S rRNA, and b) shows no current drop occurred with 10 zM *E. coli* 16S rRNA.

Although the control runs with *P. putida* RNA led to no false positives, transient blockage events were observed infrequently in some cases. Previously, we hypothesized that the electric field at the pore ( $\sim 10,000$  V/cm) is strong enough to remove non-specifically bound nucleic acid (and other negatively charged species) while not removing hybridized complementary target rRNA [19, 23-25]. In addition at neutral pH, silanol groups on the glass surfaces deprotonate giving rise to a layer of fixed negative charges neutralized by free, hydrated counterions. These hydrated cations move toward the cathode resulting in an electroosmotic flow (EOF) that exerts a drag force on PNA-beads moving toward the anode. If negatively charged species bound to the PNA-beads

are removed at the pore mouth, the nearly charge neutral beads are driven away from the pore by the EOF. This active mechanism to avert false positives is a unique aspect of our detection system.

Since our detection system also does not require purification of extracted RNA to remove inhibitors of polymerases, we explored simpler approaches. We investigated RNA extraction at alkaline pH followed by neutralization and simple, 0.02- $\mu\text{m}$  filtration. Rapid extraction under alkaline conditions resulted in higher RNA yield than with the Qiagen kit, but at lower purity (Table 3.1).

**Table 3.1.** RNA extraction time, yield, estimated 16S rRNA concentration and purity using the Qiagen kit compared to the alternate alkaline lysis/neutralization/filtration approach.

		RNeasy Kit	Alkaline Extraction
Extraction Time		>2 Hours	<10 Minutes
Yield (ng/ $\mu\text{L}$ )	<i>E. coli</i>	~200	~300-500
	<i>P. putida</i>	~100	~300-400
Estimated concentration of 16S rRNA (nM)	<i>E. coli</i>	~75.7	~113.5-189.2
	<i>P. putida</i>	~53.4	~160.3-213.8
Purity (A260/A280)		~2.00	1.53-1.90

To verify that our devices are still selective with preparations of reduced purity, we performed detection runs with samples at 100  $\mu\text{M}$  *E. coli* 16S rRNA generated by the alkaline extraction procedure followed by over-night hybridization. Representative data shown in Figure



3.4a and 3.4b (*P. putida* RNA control) confirm success at 100 zM, albeit against greater background noise including transient drops in ionic current. This observation may be due to the increased impurity of the RNA preparation leading to more nonspecific binding. One interesting point is that 3 of the detection events shown were composed of multiple small step changes of <2 nA (Fig. 3.4a), which we hypothesize are due to the accumulation of multiple beads at the pore mouth.

In an effort to further streamline the detection protocol through a more rapid hybridization step, a ~2-layer bed of PNA-beads was first deposited on the membrane of Vivaspin centrifuge filter followed by filtration of the RNA preparation produced using alkaline solution lysis. We hypothesized that better interfacial contact between PNA-beads and target RNA would enhance hybridization kinetics. As shown in Figure 3.4c and 3.4d, detection of 100 zM *E. coli* 16S rRNA was achieved with this ~10-minute hybridization protocol and no false positives were observed with the *P. putida* RNA preparation.

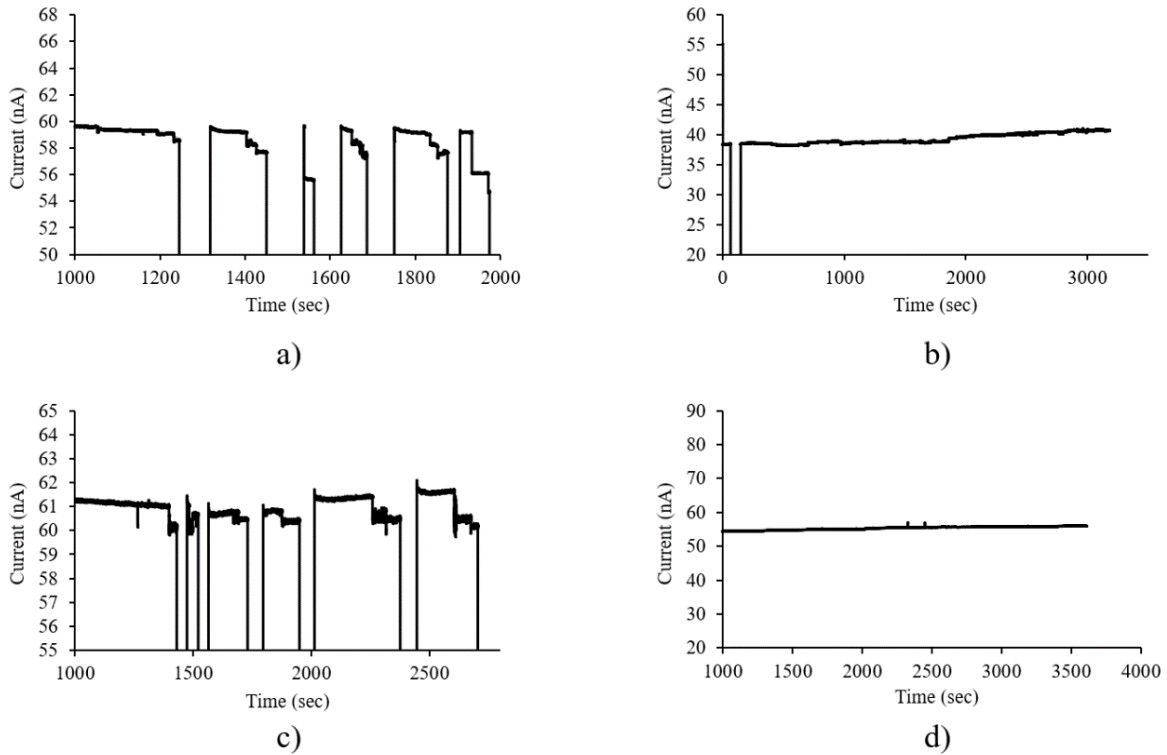


**Figure 3.4.** I) 820-nm carboxylic beads tests with alkaline extraction and over-night hybridization a) shows repeated, consistent current drop in a concentration of 100 zM of *E. coli* 16S rRNA, and b) shows that no current drop occurred for 10 fM of *P. putida* 16S rRNA. II) 820-nm carboxylic beads tests with alkaline extraction and kinetic enhanced hybridization c) shows repeated, consistent current drop in a concentration of 100 zM of *E. coli* 16S rRNA, and d) shows that no current drop occurred for 100 fM of *P. putida* 16S rRNA.

### 3.4 Conclusion

Using our novel glass chip detection system, an LOD of ~100 zM *E. coli* 16S rRNA was achieved and no false positives were observed with *P. putida* RNA. Further, this performance level also was attained with a simplified alkaline solution lysis and RNA extraction method followed by kinetically enhanced hybridization, which reduced the overall detection time from ~10 hours to ~30 minutes. These results suggest that our glass nanopore detection technology could be utilized for development of POC pathogen detection systems that are competitive with those dependent on nucleic acid amplification.

### 3.5 References

1. Mauk, M.G., et al., *Simple Approaches to Minimally-Instrumented, Microfluidic-Based Point-of-Care Nucleic Acid Amplification Tests*. Biosensors (Basel), 2018. **8**(1).
2. Ng, L.K. and I.E. Martin, *The laboratory diagnosis of Neisseria gonorrhoeae*. Can J Infect Dis Med Microbiol, 2005. **16**(1): p. 15-25.
3. Cristillo, A.D., et al., *Point-of-Care Sexually Transmitted Infection Diagnostics: Proceedings of the STAR Sexually Transmitted Infection-Clinical Trial Group Programmatic Meeting*. Sex Transm Dis, 2017. **44**(4): p. 211-218.
4. Najari, A., et al., *Reagentless ultrasensitive specific DNA array detection based on responsive polymeric biochips*. Anal Chem, 2006. **78**(22): p. 7896-9.
5. Nam, J.M., S.I. Stoeva, and C.A. Mirkin, *Bio-bar-code-based DNA detection with PCR-like sensitivity*. J Am Chem Soc, 2004. **126**(19): p. 5932-3.
6. Taton, T.A., C.A. Mirkin, and R.L. Letsinger, *Scanometric DNA array detection with nanoparticle probes*. Science, 2000. **289**(5485): p. 1757-60.
7. Thaxton, C.S., et al., *A bio-bar-code assay based upon dithiothreitol-induced oligonucleotide release*. Anal Chem, 2005. **77**(24): p. 8174-8.
8. Liu, Y.J., et al., *Magnetic bead-based DNA detection with multi-layers quantum dots labeling for rapid detection of Escherichia coli O157:H7*. Biosens Bioelectron, 2008. **24**(4): p. 558-65.
9. Kim, G.Y. and A. Son, *Development and characterization of a magnetic bead-quantum dot nanoparticles based assay capable of Escherichia coli O157:H7 quantification*. Anal Chim Acta, 2010. **677**(1): p. 90-6.

10. Zhou, J., Q.X. Wang, and C.Y. Zhang, *Liposome-quantum dot complexes enable multiplexed detection of attomolar DNAs without target amplification*. *J Am Chem Soc*, 2013. **135**(6): p. 2056-9.
11. Spain, E., et al., *Detection of sub-femtomolar DNA based on double potential electrodeposition of electrocatalytic platinum nanoparticles*. *Analyst*, 2013. **138**(15): p. 4340-4.
12. Li, C., et al., *One-Step Modification of Electrode Surface for Ultrasensitive and Highly Selective Detection of Nucleic Acids with Practical Applications*. *Anal Chem*, 2016. **88**(15): p. 7583-90.
13. Kim YJ, J.J., Li H, Yampara-Iquise H, Zheng G, Carson CA, Cooperstock M, Sherman M, Yu Q, *Three-dimensional (3-D) microfluidic-channel-based DNA biosensor for ultrasensitive electrochemical detection*. *Journal of Electroanalytical Chemistry*, 2013. **702**: p. 72-78.
14. Hu, Q., et al., *Electrochemical DNA Biosensing via Electrochemically Controlled Reversible Addition-Fragmentation Chain Transfer Polymerization*. *ACS Sens*, 2019. **4**(1): p. 235-241.
15. Chen, C.P., et al., *Ultrasensitive in situ label-free DNA detection using a GaN nanowire-based extended-gate field-effect-transistor sensor*. *Anal Chem*, 2011. **83**(6): p. 1938-43.
16. Ramnani P, G.Y., Ozsoz M, Mulchandani A, *Electronic detection of microRNA at attomolar level with high specificity*. *Anal Chem*, 2013. **85**: p. 8061-8064.
17. DeBlois RW, B.C., *Counting and Sizing of Submicron Particles by the Resistive Pulse Technique*. *Review of Scientific Instruments*, 1970. **41**: p. 909-916.

18. Rahman, M., et al., *Optical trapping assisted detection rate enhancement of single molecules on a nanopore optofluidic chip*. *Optica*, 2019. **6**(9): p. 1130-1131.
19. Koo, B., et al., *Amplification-free, sequence-specific 16S rRNA detection at 1 aM*. *Lab Chip*, 2018. **18**(15): p. 2291-2299.
20. Chernesky, M., et al., *Head-to-head comparison of second-generation nucleic acid amplification tests for detection of Chlamydia trachomatis and Neisseria gonorrhoeae on urine samples from female subjects and self-collected vaginal swabs*. *J Clin Microbiol*, 2014. **52**(7): p. 2305-10.
21. Stender, H., et al., *Rapid detection, identification, and enumeration of Escherichia coli cells in municipal water by chemiluminescent in situ hybridization*. *Appl Environ Microbiol*, 2001. **67**(1): p. 142-7.
22. Rogacs, A., Y. Qu, and J.G. Santiago, *Bacterial RNA extraction and purification from whole human blood using isotachopheresis*. *Anal Chem*, 2012. **84**(14): p. 5858-63.
23. Esfandiari, L., et al., *PCR-Independent Detection of Bacterial Species-Specific 16S rRNA at 10 fM by a Pore-Blockage Sensor*. *Biosensors (Basel)*, 2016. **6**(3).
24. Esfandiari, L., et al., *Sequence-specific DNA detection at 10 fM by electromechanical signal transduction*. *Anal Chem*, 2014. **86**(19): p. 9638-43.
25. Esfandiari, L., H.G. Monbouquette, and J.J. Schmidt, *Sequence-specific nucleic acid detection from binary pore conductance measurement*. *J Am Chem Soc*, 2012. **134**(38): p. 15880-6.

## Chapter 4: Detection of *E. coli* spiked in sterile pooled human urine

### Abstract

With the more efficient RNA extraction and hybridization approaches described in previous work, 100 zM detection of *E. coli* 16S rRNA was achieved with our glass nanopore-based detector. However, it is important to study the performance of our detector when used with samples in complex media (*i.e.*, urine) before we move into real clinical samples. *E. coli* spiked into sterile pooled human urine was therefore used as a model system. Initial tests with samples of *E. coli* in urine and blank urine controls suggested that noisy data and false positives could be caused by phospholipids commonly found in human urine. Lipase from *Mucor miehei* was added to the lysate to address this issue. The same LOD of 100 zM attained previously was achieved after 30 minutes of 0.25 U lipase pretreatment. These preliminary tests implied that sample cleanup processes in addition to filtration is required after alkaline extraction. For more consistent results, we applied rapid commercial RNA extraction kits followed by the same kinetically enhanced hybridization step in our future work with more realistic pathogen samples, such as *N. gonorrhoeae* in urine samples.

### 4.1 Introduction

Since our ultimate goal is to engineer a NA amplification-free detection system for point-of-care (POC) applications, it is necessary to study the performance of our detector in complex media. Urine is one of the most important complex clinical media that can be used to detect and manage a wide range of disorders, such as urinary tract infections, kidney disease or diabetes. Studies have suggested that uropathogenic *E. coli* can be distinguished from other bacteria common to the urinary tract based on 16S rRNA, and therefore *E. coli* in sterile human urine was

used to study and optimize our detection system.[1-3] Our target LOD was  $\leq 10$  CFU/mL. Successful completion of this study will suggest that our detector has the potential for detecting more threatening pathogens, such as *N. gonorrhoeae* in actual clinical samples.

## 4.2 Method and materials

Materials and experimental methods were the same as described in Chapter 2. The additional step was to spike sterile pooled human urine (BioIVT, Westbury, NY) with cultured bacteria. After the bacteria were cultured to log phase, viable cell concentration was determined by serial dilution and colony counts on agar plates. *E. coli* and *P. putida* were spiked into 10 mL of sterile pooled human urine to final concentrations of 10 CFU/mL and 1000 CFU/mL, respectively. Next, 1 mL urine samples were transferred into 2 mL of 0.2 M NaOH (pH  $\sim 13$ ) for bacterial lysis. After a 1 minute of incubation, 150  $\mu$ L of the mixture was added to 300  $\mu$ L of 0.2 M Tris-HCl (pH  $\sim 4.5$ ) to neutralize the pH and therefore to stop the lysis. [4] A 0.02  $\mu$ m filter was used to remove the large cell debris that could potentially cause blockage of the nanopore and false positive signals. The purity of the extracted RNA was measured using a Thermo Scientific Nanodrop 2000 and is reported in Table 4.1.

## 4.3 Results and Discussion

With the same alkaline extraction described in chapter 2, the purity of RNA from bacteria-urine mixture was significant lower compared to the result we obtained in the previous chapter, as shown in Table 4.1. For case A, bacterial cultures were pelleted out prior to the alkaline cell lysis, which minimized the impurity from culture medium (*i.e.*, soy broth and nutrient media). For case B, since we aimed to study the impact of urine on the nanopore detection system, bacterial species were spiked into sterilized human urine followed directly by the alkaline cell lysis. Therefore, it

was hypothesized that urine media accounted for the decrease in purity of the extracted RNA. Tests with samples from case B were performed, and the results are shown as Figure 4.1.

**Table 4.1.** Comparison of RNA purity between pelleted bacterial culture (Case A) and bacteria-urine mixtures (Case B) using alkaline extraction

	Purity (A260/A280)
Case A	1.53-1.90
Case B	1.31-1.51

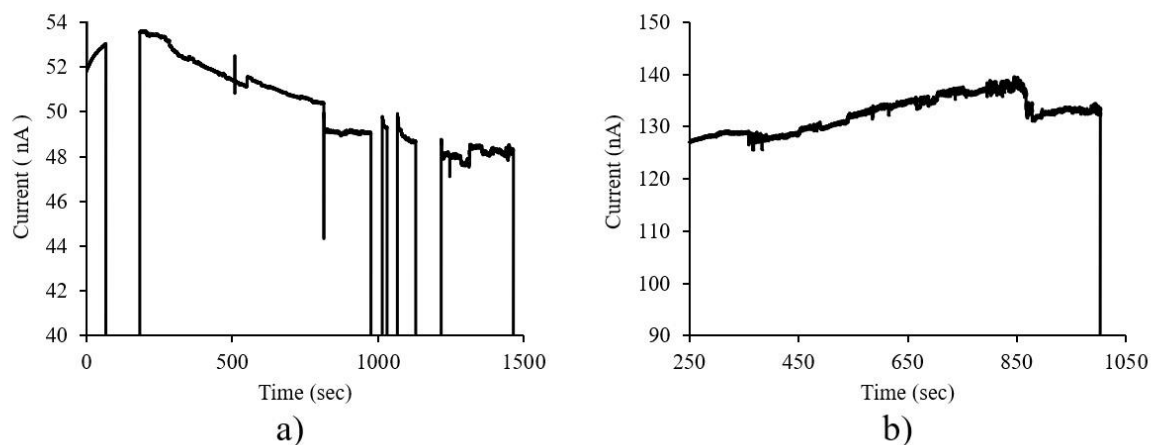


**Figure 4.1.** 820-nm carboxylic beads tests with alkaline extraction and kinetic enhanced hybridization a) shows unrepeatable permanent current drops for 10 CFU/mL of *E. coli* in sterilized human urine, and b) shows a false positive for 1000 CFU/mL of *P. putida* in sterilized human urine.

In the test with *E. coli* in sterilized human urine, a current drop was observed. However, the current could not be recovered after the voltage was reversed. Furthermore, the current was unstable with frequent transient blockages. In the negative control with *P. putida*, a permanent current drop was observed as a false positive. To further investigate the reasons for the noisy data



and false positives, we applied blank human urine to our detection system, and we observed a quick, large, and repeated current drop, as shown in Figure 4.2.

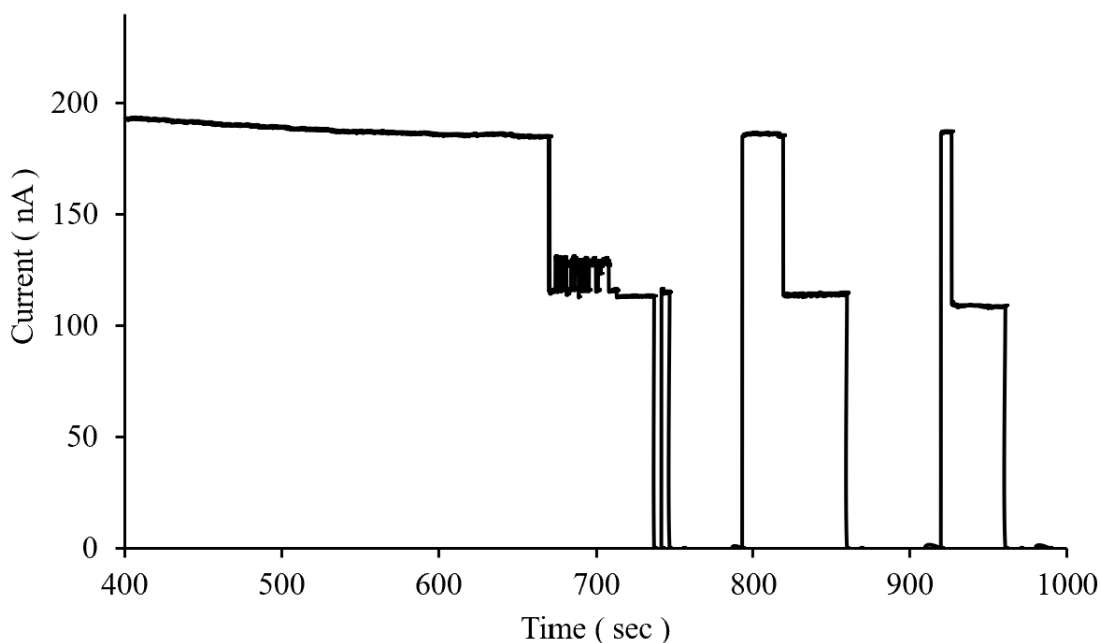
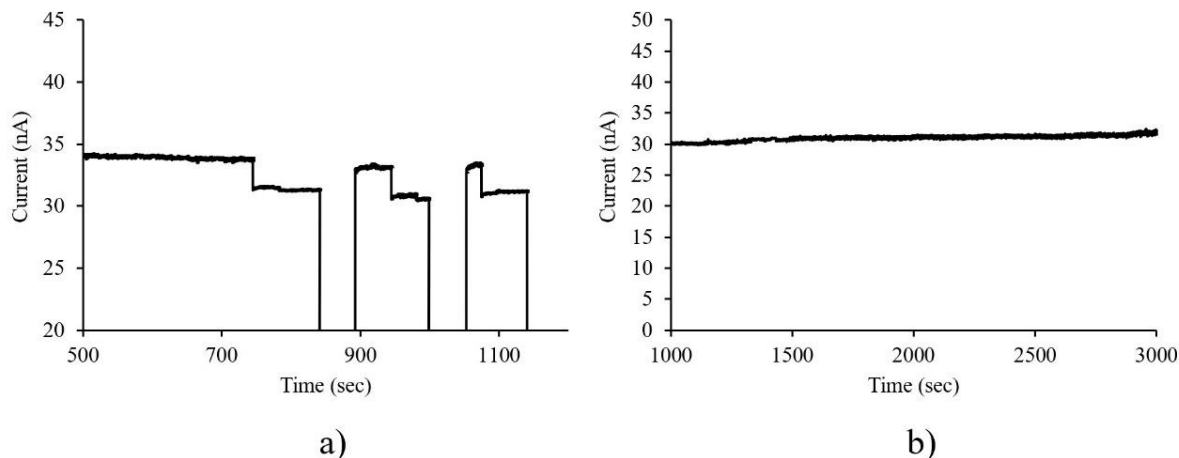


Figure 4.2. Blank human urine test shows repeatable permanent current drops.

Since urine contains a great amount of lipid/phospholipids, it might form large negatively charged liposomes. [5, 6] Therefore, we hypothesized that lipid/phospholipids broke down into smaller pieces during the filtration, and right after filtration these smaller pieces reassembled into larger liposomes that blocked the nanopore. To address this problem, we introduced lipase (from *Mucor miehei*) to degrade lipid/phospholipids and prevent the further formation of large lipid aggregates. [7] Initially, 0.25 U of lipase was added to the lysate followed by an incubation of 30 minutes and the preliminary data is showed in Figure 4.3.



**Figure 4.3.** 820-nm carboxylic beads tests with alkaline extraction, lipase treatment, and kinetic enhanced hybridization a) shows repeated, consistent current drops for 10 CFU/mL of *E. coli* in sterilized human urine, and b) shows that no false positive for 1000 CFU/mL of *P. putida* in sterilized human urine.

Clearly, our NA-based nanopore detector with alkaline extraction and kinetically enhanced hybridization was applicable for detecting bacterial species in complex media, but an additional cleanup process prior to filtration was required. In our case, lipase treatment helped resolve the problem of the noisy data and false positives, but the additional 30 minutes is lengthy for POC applications. Attempts were made to reduce the time usage by increasing the amount of lipase. However, false positives occurred again as we increased the amount of lipase to 0.5 U, which suggested that lipase itself could be an impurity that causes false positives. Since we believed it would be more important to demonstrate a stable detection of pathogen in human urine, we stepped back to use of rapid commercial RNA extraction kits, such as the Direct-zol RNA Miniprep Kits from ZYMO Research, to achieve more consistent results. But it is still suggested to investigate a faster way to clean up the urine sample without introducing new impurities. The study done by Cherif show that a high pH lipase could be produced by *Staphylococcus* sp. Stain, and this lipase have been

shown with high activity at pH 12. So, in the future we might be able to incorporate small amount of this lipase into our alkaline lysis mixture. [8]

#### 4.4 Conclusion

In this work, we successfully detected 10 CFU/mL of *E. coli* spiked in sterilized human urine with alkaline extraction followed by lipase cleanup. These preliminary results suggested that our NA-based nanopore detector has the potential to detect pathogens in urine samples. While resolving to further investigate faster and more robust sample cleanup, we settled on using Direct-zol RNA Microprep Kits from ZYMO Research followed by the same kinetically enhanced hybridization in our immediate future work.

#### 4.5 Reference

1. Liao, J.C., et al., *Use of electrochemical DNA biosensors for rapid molecular identification of uropathogens in clinical urine specimens*. J Clin Microbiol, 2006. **44**(2): p. 561-70.
2. Mohan, R., et al., *Clinical validation of integrated nucleic acid and protein detection on an electrochemical biosensor array for urinary tract infection diagnosis*. PLoS One, 2011. **6**(10): p. e26846.
3. Sun, C.P., et al., *Rapid, species-specific detection of uropathogen 16S rDNA and rRNA at ambient temperature by dot-blot hybridization and an electrochemical sensor array*. Mol Genet Metab, 2005. **84**(1): p. 90-9.
4. Rogacs, A., Y. Qu, and J.G. Santiago, *Bacterial RNA extraction and purification from whole human blood using isotachopheresis*. Anal Chem, 2012. **84**(14): p. 5858-63.
5. Bouatra, S., et al., *The human urine metabolome*. PLoS One, 2013. **8**(9): p. e73076.

6. Kim, H., E. Ahn, and M.H. Moon, *Profiling of human urinary phospholipids by nanoflow liquid chromatography/tandem mass spectrometry*. Analyst, 2008. **133**(12): p. 1656-63.
7. Mutua, L.N., Akoh, C.C, *Lipase-catalyzed modification of phospholipids: Incorporation of n-3 fatty acids into biosurfactants*. J Am Oil Chem Soc, 1993. **70**: p. 125-128.
8. Cherif, S., Mnif, S., Hadrich, F. et al. *A newly high alkaline lipase: an ideal choice for application in detergent formulations*. Lipids Health Dis, 2011. 10, 221

## **Chapter 5: An amplification-free, 16S rRNA test for *Neisseria gonorrhoeae* in urine**

Chapter 5 is a manuscript submitted to Sensors & Diagnostics, the Royal Society of Chemistry and is currently under review.

### **Abstract**

An amplification-free, nanopore-based nucleic acid detection platform has been demonstrated for rapid, 16S rRNA sequence-specific detection of *Neisseria gonorrhoeae* at 10-100 CFU/mL in human urine against background bacterial flora at 1000 CFU/mL. Gonorrhea is a very common notifiable communicable disease, antibiotic resistant strains have emerged, and the rate of reported gonococcal infections continues to increase. Since rapid clinical identification of bacterial pathogens in clinical samples is needed to guide proper antibiotic treatment and to control disease spread, it is important to engineer rapid, sensitive, selective, and inexpensive point-of-care (POC) diagnostic devices for pathogens such as *N. gonorrhoeae*. Our detector technology is based on straightforward conductometric detection of sustained blockage of a glass nanopore. Charge neutral, complementary peptide nucleic acid probes are conjugated to polystyrene beads to capture *N. gonorrhoeae* 16S rRNA selectively. In the presence of an electric field applied externally through a glass nanopore, the PNA-microbead conjugates that acquire substantial negative charge upon target hybridization are driven to the smaller diameter nanopore. At least partial blockage of the nanopore results in a sustained drop in ionic current that can be measured easily with simple electronics. The ability to detect *N. gonorrhoeae* over the range of 10 to 100 CFU/mL spiked in human urine was demonstrated successfully with estimated sensitivity and specificity of ~98% and ~100%, respectively. No false positives were observed for the control group of representative background flora (*E. coli*, *K. pneumoniae*, and *E. faecalis*) at 1000 CFU/mL. Also, *N. gonorrhoeae* at 50 CFU/mL was successfully detected against 1000 CFU/mL of background flora

in urine. These results suggest that this amplification-free technology may serve as the basis for rapid, inexpensive, low-power detection of pathogens in clinical samples at the POC.

## 5.1 Introduction

Gonorrhea is the second most common notifiable sexually transmitted infection in the US, and its prevalence has been increasing. [1] A total of 677,769 cases of gonorrhea were reported to the US Centers for Disease Control and Prevention (CDC) in 2020 out of an estimated 1.6M new infections that occur each year in the US. [1, 2] Since the historic low in 2009, reports of gonorrhea infection have increased 111%. [1] Alarming, strains of the gram-negative bacterium responsible for gonorrhea infections, *Neisseria gonorrhoeae*, have developed antibiotic resistance; and about half of all gonorrhea infections reported in 2020 were caused by an antibiotic resistant strain. [1] Only one recommended treatment remains: the cephalosporin, ceftriaxone. [2] Unfortunately, the infection often is asymptomatic in women, and if untreated, pelvic inflammatory disease leading to ectopic pregnancies and infertility can result. [3] Currently, the CDC recommends that all sexually active women under age 25, as well as sexually active gay or bisexual men, be tested each year.[3] In order to guide proper usage of antibiotics, to perform timely treatment, and to curtail disease spread, rapid, inexpensive point-of-care (POC) diagnostic tests are needed urgently.

The historical method for *N. gonorrhoeae* detection in a clinical sample has long entailed culturing; however, at least a day is required for results that must be generated by skilled technicians. [4] Microscopic examination of urethral smears also can be used to provide evidence of infection, but the reliability of this diagnostic approach depends strongly on the quality of the specimen and the experience of the microscopist. [4] Currently, nucleic acid amplification tests (NAATs) are the preferred methods for gonorrhea diagnostic detection due to sensitivities >90% and very high specificities of ~99%. [5] However, most NAATs are conducted in the clinical

laboratory where the turnaround time also is a day or longer, and these complex systems must be operated by trained personnel. POC NAATs have emerged on the market recently (*i.e.*, Binx io, Visby Medical Sexual Health Test), [6, 7] but an external power source is required for these complex devices that entail nucleic acid (NA) isolation to high purity for removal of polymerase inhibitors; tight control of complex reaction steps involving expensive, perishable reagents (*e.g.*, primers, polymerase, and nucleotides); optical or electrochemical means to detect amplicons; and assay times of ~15-30 minutes. An ideal NA-based POC diagnostic system would exhibit an assay time of ~5 minutes, would be battery powered and completely portable, would be inexpensive (~\$20/test), and would provide competitive sensitivity and specificity of  $\geq 95\%$ . [8, 9]

The need for more optimal POC diagnostic tests has provided impetus for a number of studies focused on simpler, yet powerful, amplification-free, NA-based detection approaches. The “gold standard” limits of detection (LODs) of commercial clinical laboratory-based NAATs available for *N. gonorrhoeae* in urine in the ~1–100 CFU/mL range are reflective of clinical need and correspond to NA LODs at the single-digit aM ( $10^{-18}$  M) level.<sup>10</sup> Over the past 10 years or so, many reports, including ours, have appeared describing NA amplification-free systems exhibiting these very low LODs for NAs of specific sequence.[10, 11] Our system utilized here relies on the use of peptide nucleic acid (PNA) capture probes.[12] PNA is an uncharged polyamide analog to DNA/RNA that we bind covalently to carboxyl-functionalized microbeads to form nearly charge neutral bead-probe conjugates. When the neutral PNA-microbead hybridizes target NA, it gains substantial negative charge thereby making it mobile in an electric field. If the negatively charged PNA-microbeads with hybridized target NA are directed to a glass nanopore of lesser diameter, they will at least partially block it, resulting in a sustained, easily measured drop in ionic current. In previous work, our group has successfully demonstrated the detection of *E. coli* rRNA at a

concentration of 1 aM against a  $10^6$ -fold background of *P. putida* RNA and *E. coli* at 10 CFU/mL against a  $10^6$ -fold background of viable *P. putida*. [11] However, few NA amplification-free detection schemes, including ours, had been tested with clinical, or even mock clinical, specimens. [10]

## 5.2 Methods and materials

### 5.2.1 Reagents

Carboxyl-functionalized, 820 nm-dia. polystyrene microspheres and Vivaspin® 2 mL ultrafiltration devices were purchased from Bangs Laboratories, Inc. (Fishers, IN). 1-Ethyl-3-(3-dimethylaminopropyl)carbodiimide hydrochloride (EDC) was obtained from ThermoFisher Scientific (Waltham, MA). 2-(*N*-Morpholino)ethanesulfonic acid (MES), methoxypolyethylene glycol amine (mPEG-amine) and ethanolamine were purchased from Sigma-Aldrich (St. Louis, MO). Peptide nucleic acid (PNA) probes were synthesized by PNA Bio (Thousand Oaks, CA) and arrived as >95% HPLC-purified, lyophilized powders. *E. coli* (ATCC 25922), *P. putida* (ATCC 12633), spy broth and nutrient broth were purchased from American Type Culture Collection (Manassas, VA). Direct-zol RNA Miniprep kits and TRI Reagent were purchased from Zymo Research (Irvine, CA). Two mm-diameter, 4 mm-long Ag/AgCl pellet electrodes were purchased from A-M systems, Inc. (Carlsborg, WA). GE Healthcare Life Sciences Anotop 25 syringe filters (25 mm-diameter, 0.02  $\mu\text{m}$  pore) were supplied by Genesee Scientific (San Diego, CA).

### 5.2.2 Detector assembly

Glass chips (1 cm  $\times$  1 cm) were micromachined from 4-in. borosilicate glass wafers (Plan Optik, Elsoff, Germany) as described earlier. [11] A  $\sim 0.25 \text{ mm}^2$ , 1  $\mu\text{m}$ -thick membrane was etched



in the center of the chip and a ~500 nm nanopore was milled in the center of the membrane with a focused ion beam (FEI Nova 600 Nanolab DualBeam SEM/FIB). These glass chips were sandwiched between two, custom-machined Teflon chambers (each measuring 6 mm × 6 mm × 8 mm, 216 μL) with cast polydimethylsiloxane (PDMS) seals (Fig. 5.1). A 4 mm-diameter hole drilled through the chamber walls facing the glass chip permitted buffer access on either side of the chip. A Ag/AgCl pellet electrode was placed in each, buffer-filled chamber, and voltage was controlled and current monitored using a Versatile Multichannel Potentiostat (model VMP3) equipped with the ‘p’ low current option and N’Stat box driven by EC-LAB software (Bio-Logic USA, LLC, Knoxville, TN). This assembly constituted our detection system for target *N. gonorrhoeae* 16S rRNA hybridized to PNA probe conjugated to microspheres (see below).

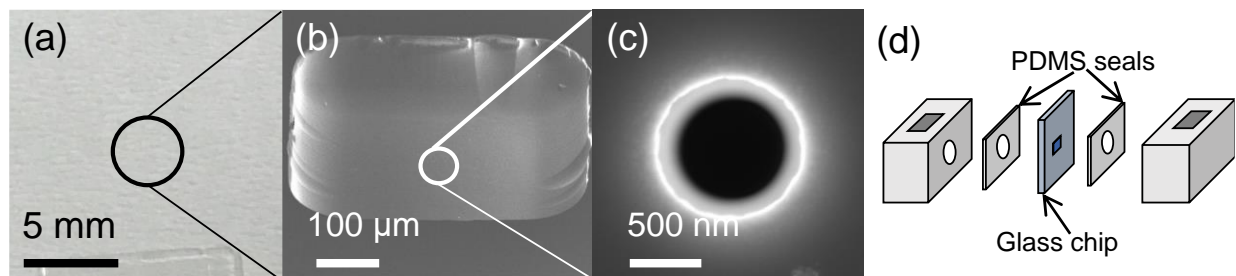


Figure 5.1. Glass chip and detector assembly. a) The 1 cm × 1 cm chip with ~1 μm-thick membrane and pore in the center. b) Micrograph of the ~1 μm-thick membrane at the chip center. c) Micrograph of the ~500 nm pore at the center of the glass membrane. d) The glass chip sandwiched between Teflon chambers (6 mm × 6 mm × 8 mm).

### 5.2.3 Coupling PNA probe to microspheres

The complementary PNA probe sequence with PEG linker for detecting *N. gonorrhoeae* 16S rRNA consisted of NH<sub>2</sub>-(CH<sub>2</sub>CH<sub>2</sub>OCH<sub>2</sub>CH<sub>2</sub>OCH<sub>2</sub>CO)<sub>6</sub>- TTG CCA ATA TCG GCG GCC. [13] In order to prepare microspheres to be conjugated with PNA, one μL of 820 nm-diameter carboxylic group-functionalized polystyrene microspheres, at a concentration of ~3.25 × 10<sup>11</sup>/mL, was suspended and washed three times in 100 mM MES buffer (pH 4.5). For each wash step, after

centrifugation at 14,000 rpm for 15 minutes, the sedimented pellet microspheres were resuspended in fresh MES buffer. After the third wash, the microbeads were re-suspended in 600  $\mu$ L of MES buffer, and EDC (200 mM final concentration) was added to the suspension to serve as a crosslinker between the carboxyl groups on the polystyrene microbeads and the terminal primary amine groups appended on the PNA probes. This preparation was incubated for 15 minutes at 50 °C. Immediately afterward, 1.14 nmol of the PNA target probe was added followed by incubation for an additional two hours at 50 °C. Next, mPEG-amine was added to a final concentration of 100 mM followed by incubation for another hour at 50 °C. This latter conjugation step was added to inhibit microbead aggregation. Finally, ethanolamine was added to a final concentration of 138 mM and incubated for yet another hour at 50 °C. Ethanolamine was added to fully cap any remaining carboxyl groups, thereby ensuring that the PNA-conjugated microbeads were nearly charge neutral. After completion of microbead surface modification, the beads were washed three times with 0.4 $\times$  SSC buffer (60 mM NaCl, 6 mM trisodium citrate, and 0.1% Triton X-100, pH 8). Each wash was conducted for 15 minutes at 14,000 rpm in microfuge tubes. One fourth of the final product was set aside for zeta potential measurements, while the rest of the PNA-beads were stored in hybridization buffer at room temperature (10 mM NaCl, 25 mM Tris-HCL, pH 7). The zeta potential was measured for modified microbeads suspended in the testing buffer (10 nM KCl, 5.5 mM HEPES, 0.01% Tween-80, pH 7) using a Malvern Zetasizer Nano ZS (Malvern Instruments Ltd, Worcestershire, England). A zeta potential in the negative single-digit mV range was taken as evidence of successful microbead surface modification.

#### 5.2.4 RNA extraction

*N. gonorrhoeae* (ATCC 43069) frozen stock was subcultured onto chocolate agar. Agar plates were incubated at 35 °C with 5% CO<sub>2</sub> for 16-18 hrs. The bacterium was cultured in ATCC

814 medium to a McFarland standard 0.5 corresponding to  $\sim 1.5 \times 10^8$  CFU/mL. The culture then was serially diluted in 0.85% saline to achieve the desired concentrations for spiking into sterilized pooled human urine (BioIVT, Westbury, NY). The background bacterial flora including *E. coli*, *K. pneumoniae*, and *E. faecalis* served as negative controls. The protocols for use of the Direct-zol RNA Miniprep kit and TRI Reagent (Zymo Research, Irvine, CA) were followed for total RNA extraction and purification. Each extraction began with 1 mL of human urine previously spiked with 10-100 CFU/mL of *N. gonorrhoeae*, 1000 CFU/mL of background flora, or 10-100 CFU/mL of *N. gonorrhoeae* and 1000 CFU/mL of background flora. Extracted total RNA was eluted into 100  $\mu$ L of RNase-free purified water and used within  $\sim 1$ -2 hours.

#### 5.2.5 Hybridization of RNA to PNA-bead conjugates

Hybridization was accomplished in Vivaspin® 2 mL ultrafiltration devices with 0.02- $\mu$ m-diameter membranes. Bead-PNA conjugates in 600  $\mu$ L hybridization buffer (see above) were transferred to Vivaspin® devices and spun at 1000 rpm for 5 minutes to form a compact bed of the conjugates on the membrane surface. Subsequently, extracted RNA from *N. gonorrhoeae* spiked in human urine was added to the loaded Vivaspin® device and spun at 1000 rpm for 5 minutes to facilitate intimate contact and hybridization of target 16S rRNA with the previously deposited bead-PNA conjugates. Finally, after two rounds of wash with hybridization buffer in the Vivaspin®, hybridized beads were collected in hybridization buffer by reverse spinning the loaded Vivaspin® devices.

#### 5.2.6 Sample detection

Prior to the injection of a sample, the open current was measured to verify the integrity of the glass chips. Depending on the exact nanopore size, clean glass chips had typical open currents of 35 nA to 100 nA. After undergoing the hybridization procedure, bead-PNA conjugates

potentially bound with target *N. gonorrhoeae* 16S rRNA were injected into the detector chamber contacting the smooth backside (opposite the etched well) of the glass chip. After bead sample addition, a potential of 1.5 V was imposed, and the current was monitored for a sustained, ionic current drop that would signal detection of target 16S rRNA. After each detection signal (indicated by sustained ionic current drop of ~50 s) was observed, the polarity of the electronic field was reversed to -1.5 V to attempt to unblock the pore. After ~1 min of reversed polarity, the field was flipped back to 1.5 V to confirm baseline current recovery and detection signal reproducibility

### **5.3 Results and Discussion**

Forty-four samples of *N. gonorrhoeae* spiked in human urine over the 10-100 CFU/mL concentration range (14 at 10 CFU/mL, 10 each at 50 and 100 CFU/mL, and 10 at 50 CFU/mL against representative bacterial flora at 1000 CFU/mL) were processed and tested as described above. The bacterial flora control representative of microbes frequently present in human urine included *E. coli*, *K. pneumoniae*, and *E. faecalis*. Out of these 44 trials, only one false negative was observed at 50 CFU/mL. No positive detection results were recorded for any of 10 samples of the background flora alone at a concentration of 1000 CFU/mL in human urine, which served as a negative control. Sample data showing easily recognized, reproducible detection events as well as the lack of response to the negative control is presented as Fig. 5.2, and the complete results are summarized in Table 5.1.

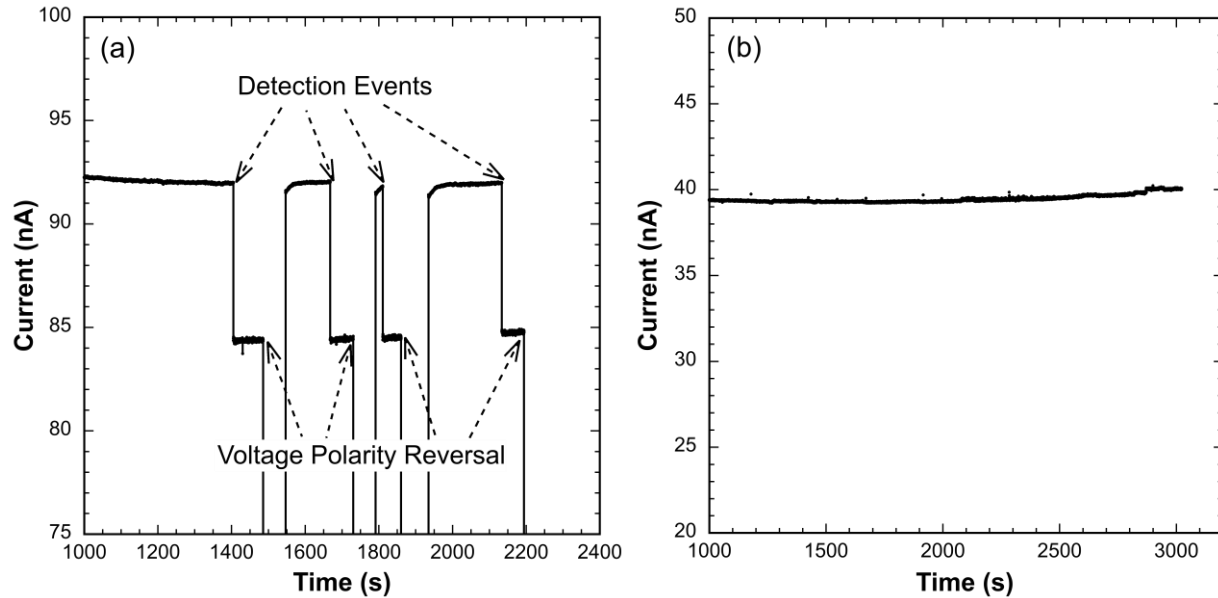


**Figure 5.2.** Detector current response to the presence of target *N. gonorrhoeae* 16S rRNA and the lack of response to RNA extracted from background bacterial flora alone. (a) Reproducible, sustained current signal step reductions in response to the presence of PNA-beads with hybridized target 16S rRNA extracted from *N. gonorrhoeae* at 10 CFU/mL in human urine. The applied voltage for detection events was 1.5 V. After a sustained current signal of ~50 s, the voltage polarity was reversed temporarily to -1.5 V to drive bead complexes away from the pore before demonstrating signal reversibility by reimposing a potential of 1.5 V. (b) No current signal in response to the presence of PNA-beads hybridized with RNA extracted from background bacterial flora spiked at 1000 CFU/mL in human urine (negative control).

**Table 5.1.** Summary of *N. gonorrhoeae* (NG) detection data over a concentration range of 10-100 CFU/mL in human urine

Sample	Agreement w/Expected result*
10 CFU/mL	14/14
50 CFU/mL	9/10
100 CFU/mL	10/10
50 CFU/mL + 1000 CFU/mL Flora *	10/10
1000 CFU/mL Flora *	10/10
Total agreement	53/54 (98.1%)

\*(number of expected test results) / (number of tests)

\*\*Background flora included *E. coli*, *K. pneumoniae*, and *E. faecalis*. Background flora also served as negative control.

The data presented in Table 1 provide the basis for preliminary estimates of sensitivity and specificity of ~98% and ~100%, respectively, for detection of *N. gonorrhoeae* over the range of 10 to 100 CFU/mL when spiked in sterile pooled human urine. Note that the first detection event for true positive cases, indicated by the first sustained ionic current drop, occurred from 500 seconds to 1500 seconds. Absence of ionic current drop for over 3000 seconds constituted negative detection (likely an extreme waiting period based on many test runs), and only one false negative was observed at 50 CFU/mL. Since 50 CFU/mL is well above the detection limit of our device,

we suspect that RNA instability may have played a role since samples were lysed at the off-campus clinical laboratory and subsequently transported on campus for testing. Nevertheless, the preliminary sensitivity and specificity data presented here compare very well to the currently preferred NAATs, both those that are lab-based and those that are designed for the POC. [6, 7]

As an amplification-free test, this technology is considerably less complex than NAATs and avoids the need for perishable reagents (*i.e.*, polymerase, primers, nucleotides). The current lab-based version of our amplification-free test with the glass nanopore detector requires ~10 minutes for RNA extraction, ~10 minutes for hybridization, and ~15 minutes for sample detection, which makes it competitive in overall assay time with many fully automated NAATs. However, the detection chamber in a microfluidic device under development is reduced  $\sim 10 \times$  in characteristic dimension thereby dramatically reducing the transit time of bead-PNA conjugates with hybridized target to the glass nanopore detector. In the near future, we anticipate reporting on the extensive time savings achieved with our glass chip detectors integrated into a complete, low-power automated system that also includes frontend sample processing and hybridization, as well as an order-of-magnitude reduction in detection chamber size.

## 5.4 Conclusions

A novel amplification-free rRNA test based on a nanopore glass detector was used successfully to assay for *N. gonorrhoeae* spiked in human urine with high sensitivity (~98%) and specificity (~100%). *N. gonorrhoeae* was detected successfully over the 10-100 CFU/mL range and against background bacterial flora at 1000 CFU/mL. These results suggest that this potentially rapid and inexpensive technology may one day prove advantageous for POC use. Indeed with further improvement in overall assay time and integration of the glass nanopore detector with automated frontend sample processing, this simple, amplification-free detection technology may

lead to rapid, inexpensive, low-power and portable POC pathogen detection devices with minimal reagent requirements.

## 5.5 References

1. CDC, Sexually Transmitted Disease Surveillance 2020, <https://www.cdc.gov/std/statistics/2020/overview.htm#Gonorrhea>, (accessed July 19, 2022).
2. Schlanger K, Kirkcaldy RD, *Rising to Meet the Programmatic Public Health Challenges of Emerging Neisseria gonorrhoeae Antimicrobial Resistance: Strengthening the United States Response to Resistant Gonorrhea*. Sex Transm Dis, 2021. 48:S91-S92.
3. CDC, Gonorrhea—CDC Detailed Fact Sheet, <https://www.cdc.gov/std/gonorrhea/stdfact-gonorrhea-detailed.htm>, (accessed July 19, 2022).
4. Ng, L.-K. and I.E. Martin, *The laboratory diagnosis of Neisseria gonorrhoeae*. Canadian Journal of Infectious Diseases and Medical Microbiology, 2005. 16(1): p. 15-25.
5. Centers for Disease, C. and Prevention, *Recommendations for the laboratory-based detection of Chlamydia trachomatis and Neisseria gonorrhoeae--2014*. MMWR Recomm Rep, 2014. 63(RR-02): p. 1-19.
6. Morris, S.R., et al., *Performance of a single-use, rapid, point-of-care PCR device for the detection of Neisseria gonorrhoeae, Chlamydia trachomatis, and Trichomonas vaginalis: a cross-sectional study*. Lancet Infect Dis, 2021. 21(5): p. 668-676.
7. Van Der Pol, B., et al., *Evaluation of the Performance of a Point-of-Care Test for Chlamydia and Gonorrhea*. JAMA Netw Open, 2020. 3(5): p. e204819.



8. Gaydos, C.A., Y.C. Manabe, and J.H. Melendez, *A Narrative Review of Where We Are With Point-of-Care Sexually Transmitted Infection Testing in the United States*. Sex Transm Dis, 2021. 48(8S): p. S71-S77.
9. Atkinson, L.M., et al., *'The waiting game': are current chlamydia and gonorrhoea near-patient/point-of-care tests acceptable to service users and will they impact on treatment?* Int J STD AIDS, 2016. 27(8): p. 650-5.
10. Cao, Y., Z. Zheng, and H.G. Monbouquette, *Nucleic acid amplification-free detection of DNA and RNA at ultralow concentration*. Curr Opin Biotechnol, 2021. 71: p. 145-150.
11. Koo, B., et al., *Amplification-free, sequence-specific 16S rRNA detection at 1 aM*. Lab Chip, 2018. 18(15): p. 2291-2299.
12. Nielsen, P.E., et al., *Sequence-selective recognition of DNA by strand displacement with a thymine-substituted polyamide*. Science, 1991. 254(5037): p. 1497-500.
13. Chui, L., et al., *A comparison of three real-time PCR assays for the confirmation of Neisseria gonorrhoeae following detection of N. gonorrhoeae using Roche COBAS AMPLICOR*. Clin Microbiol Infect, 2008. 14(5): p. 473-9.

## **Chapter 6: Amplification-free detection of 16S rRNA using a glass chip detector integrated into the lateral flow assay format**

### **Abstract**

A nucleic acid amplification-free platform integrated with the lateral flow assay (LFA) format has been demonstrated for rapid detection of 10 attomolar (aM) *Escherichia coli* 16S rRNA within 15 minutes. The ongoing COVID-19 pandemic and the public health issues revealed during this crisis have illustrated the need for rapid, convenient, and customer-affordable disease diagnostic methods that can meet point-of-care (POC) requirements with simple operating procedures. Clinical studies have shown that a substantial portion of the patient population is unwilling to wait in the clinic for more than 20 minutes for a test result; therefore, in order to address POC requirements better, an NA detection method with an assay time as short as 5 minutes has been developed. The single-use component of the system is composed of a glass chip-based nanopore detector integrated with a lateral flow membrane strip which is preloaded with polystyrene microbeads conjugated with peptide nucleic acid (PNA) probe complementary to the target 16S rRNA. A 100  $\mu$ L rRNA sample deposited on the test strip quickly flows along the LFA membrane due to capillary action, and target rRNA hybridizes with the complementary PNA probes conjugated to the preloaded microbeads. Driven by an externally applied electronic field, the PNA-microbeads with the negative charge added by the hybridized rRNA are driven to the smaller nanopore on the integrated glass chip and at least partially block it resulting in a sustained drop in ionic current. This easily measured, step change in current constitutes the signal indicating the presence of target nucleic acid. With this system, the detection of 10 aM *E. coli* 16S rRNA against 10 fM *P. putida* 16S rRNA within 15 minutes has been successfully demonstrated. Finally, our LFA device readily detected *E. coli* at 10 CFU/mL against a one-million-fold background of

viable *P. putida*. With further improvements in sensitivity and reliability, this simple, rapid, and inexpensive amplification-free technology may be promising for widespread diagnostic usage in defense of public health.

## 6.1 Introduction

The ongoing COVID-19 pandemic and the public health issues revealed during this crisis have illustrated that there is great demand for low-cost, sensitive, and robust point-of-care (POC) nucleic acid (NA) based diagnostic devices that give results in minutes. Culturing methods and laboratory-based nucleic acid amplification tests (NAATs) are authoritative diagnosis methods for most infectious diseases with high sensitivity, but both have turnaround times of one day or more. [1] This causes a problematic time gap for patients to get the optimal counseling and therapies, which is exacerbated by the need for undependable follow-up visits. To date, several NAATs have been developed for POC application. [2] These PCR-dependent POC NAATs are highly sensitive and selective compared to traditional POC immunoassays, but the NA amplification step requires precise reaction control, expensive reagents such as primers and polymerases, and added time. The overall assay time for POC NAATs is ~15-30 minutes, but it has been shown that a significant portion of the population will not wait in the clinic for test results that take this long. [3, 4] In recent years, remarkable progress has also been made in development of amplification-free NA detection with single-digit attomolar ( $10^{-18}$  M) detection limits. Optical methods are common among these amplification-free methods with utilization of nanoparticles, such as gold nanoparticles, functionalized magnetic beads or quantum dot fluorescence, as the key element to convert a selective hybridization event into an optical signal. Yet the requirement of optical components increases complexity and cost. Electrochemical approaches, such as constant potential amperometry (CPA), cyclic voltammetry (CV) and field effect transistors (FETs), also provide

ultralow concentration detection by transducing the hybridization event into an electric signal, yet additional labels and/or lengthy assay times are required for most of the schemes. [5]

Our detection system provides a simple binary yes/no response to hybridization of the sequence-specific 16S rRNA of bacterial pathogens by utilizing peptide nucleic acid (PNA), an uncharged polyamide analog to DNA/RNA. PNA is covalently bound to carboxyl-functionalized polystyrene microbeads to form neutral bead-probe conjugates. Yet when the neutral PNA-microbead conjugates hybridize with target rRNA, they gain substantial negative charge and therefore exhibit electrophoretic mobility in an electric field. If the complex is directed to a smaller diameter nanopore in a glass membrane, it will at least partially block it, resulting in a sustained drop in ionic current thereby signaling the presence of the target rRNA. In previous work, our group has successfully demonstrated the detection of 16S rRNA of *E. coli* at a concentration of 100 zM and 50 CFU/mL of *N. gonorrhoeae* against a 1000 CFU/mL background of bacterial flora. However, an average one-hour detection time was reported from sample to result due to the macro size of the experimental setup and the need for an external hybridization step. In our previous setting, the average distance for beads to travel from teflon chamber to nanopore is about 0.6 cm, therefore, it is hypothesized that reducing the travel distance for beads will help shorten the detection time. Lateral flow assay (LFA) technology presents a straightforward approach for integrating our nanopore detector into inexpensive handheld POC devices. In LFAs, liquid samples were carried by capillary flow through porous membrane strips thereby avoiding construction of complex microfluidic channels with pumps and valves. This technology has been proven highly successful and is the basis for the immunoassay-based pregnant test strips. [6-8] Therefore, we attempted to integrate our glass chip-base detector in an easily assembled LFA format prototype

that includes integration of the hybridization step by pre-depositing the PNA-beads just downstream of the sample loading area.

## 6.2 Method and Materials

### 6.2.1 Reagents

Carboxyl-functionalized, 1  $\mu\text{m}$ -dia. polystyrene microspheres were purchased from Bangs Laboratories, Inc. (Fishers, IN). (1-Ethyl-3-(3-dimethylaminopropyl)carbodiimide hydrochloride) (EDC) was obtained from ThermoFisher Scientific (Waltham, MA). 2-(*N*-Morpholino)ethanesulfonic acid (MES), methoxypolyethylene glycol amine (mPEG-amine), ethanolamine and 0.0025 mm-thick platinum foil were purchased from Sigma-Aldrich (St. Louis, MO). Peptide nucleic acid (PNA) probes were synthesized by PNA Bio (Thousand Oaks, CA) and arrived as >95% HPLC-purified, lyophilized powders. *E. coli* (ATCC 25922), *P. putida* (ATCC 12633), soy broth and nutrient broth were purchased from American Type Culture Collection (Manassas, VA). Direct-zol RNA miniprep kits were purchased from ZYMO Research (Irvine, CA). Ag/AgCl pellet electrodes of 2 mm dia. were purchased from A-M systems, Inc. (Carlsborg, WA). GE Healthcare Life Sciences Anotop 25 syringe filters (25 mm-diameter, 0.02  $\mu\text{m}$  pore) were supplied by Genesee Scientific (San Diego, CA). Fusion 5 membrane material and backing cards were purchased from Cytiva (Marlborough, MA).

### 6.2.2 Coupling PNA probe to microspheres

The target PNA probe sequence for detecting *E. coli* 16S rRNA was NH-(CH<sub>2</sub>CHOCH<sub>2</sub>CHOCH<sub>2</sub>CO)- CTC CTT CCC TCA TTT CA.[9] To prepare microspheres to be conjugated with PNA, one  $\mu\text{L}$  of 1  $\mu\text{m}$ -diameter carboxylic group-functionalized polystyrene microspheres, at a stock concentration of  $1.58 \times 10^{11}/\text{mL}$  were suspended and washed three times

in MES buffer (100 mM 2-(N-morpholino) ethanesulfonic acid, pH 4.5). For each wash step, after centrifugation at 14,000 rpm for 15 minutes, the sedimented pellet microspheres were resuspended in fresh MES buffer. After the third wash, the beads were resuspended in 600  $\mu$ L MES buffer, and EDC (200mM final concentration) was added to the suspension to serve as a crosslinker between the carboxyl groups on the polystyrene microbeads and the terminal primary amine groups on the PNA probes. This preparation was incubated at 50 °C for 15 minutes. Next, 1.14 nmol of the PNA target probe was added followed by incubation of two hours at 50 °C. To inhibit bead aggregation, mPEG-amine was added to a final concentration of 100 mM and incubated at 50 °C for one hour. Finally, ethanolamine was added to a final concentration of 138 mM and incubated at 50 °C for another hour. Ethanolamine was added to fully cap any remaining carboxyl groups, ensuring the PNA conjugated beads are near charge neutral. After the surface modification of the polystyrene microbeads, the beads were washed three times in 0.4  $\times$  SSC solution (60 mM NaCl, 6 mM trisodium citrate, and 0.1% Triton X-100, pH 8). Each wash was done at 14,000 rpm for 15 minutes. One fourth of the final product was taken for zeta potential measurement, and the rest of the beads were stored in the hybridization buffer at room temperature (10 mM NaCl, 25 mM Tris-HCL, pH 7). The zeta potential was measured with microbeads suspended in the hybridization buffer with a Malvern Zetasizer Nano ZS (Malvern Instruments Ltd, Worcestershire, England). A zeta potential in the negative single-digit mV range was taken as evidence of successful microbead surface modification.

### 6.2.3 Cell culturing and counting

*E. coli* ATCC 25922 was cultured in tryptic soy broth, and *P. putida* ATCC 12633 was cultured in ATCC nutrient broth. Both tryptic soy broth and nutrient broth were sterilized at 120 °C for 20 minutes prior to use. To initiate the bacterial culture of *E. coli* and *P. putida*, lyophilized

preparations were mixed into tryptic soy broth and nutrient broth, respectively, followed by incubation of two days. *E. coli* was cultured at 37 °C and 250 rpm, and *P. putida* was cultured at room temperature and 250 rpm. Aliquots of both cultures were stored at -80 °C to serve as inocula for future cultures. To prepare a sample for RNA extraction (see below), a small portion of frozen *E. coli* and *P. putida* were taken and mixed into 3 mL of tryptic soy broth and nutrient broth, respectively. Both *E. coli* and *P. putida* were incubated overnight under the same conditions described above. Cultured bacterial cells were then serially diluted, plated and incubated overnight for colony counting.

#### 6.2.4 RNA extraction

For the experiments to determine the limit of detection (LOD), total RNA from both *E. coli* and *P. putida* cultures were extracted separately. Prior to the extraction, 1 mL of bacterial culture was pelleted out by centrifugation. Next, 1 mL of TRI Reagent was added followed by an incubation of 5 minutes. Cell lysate including TRI reagent was transferred into Zymo-Spin™ IIIICG Column for purification, and the final RNA product was eluted into 100 µL of RNase-free purified water and used within ~1-2 hours. The concentration of the total extracted RNA was measured using a Thermo Scientific Nanodrop 2000. An A260/A280 ratio above 1.8 suggested highly purified RNA. According to previous measurements, approximately 18.2% of the total RNA is 16S rRNA for *E. coli* and 25.7% of the total RNA is 16S rRNA for *P. putida*. [10] The estimated concentration varied from ~50 nM to ~200 nM for both cultures in different trials. To verify the detection of viable cells, 10 CFU/mL of *E. coli* was mixed with 10<sup>6</sup> CFU/mL of *P. putida* prior to the total RNA extraction. Next, 1 mL of the bacterial mixture was collected into 3 mL of TRI reagent followed by the same procedure describe above. The concentration of viable cells was determined by serial dilution and colony counts on agar plates.

### 6.2.5 Lateral flow assay system assembly and sample detection

Glass chips (shown in Figure 6.1) were previously microfabricated from 4-in. borosilicate glass wafers. After a  $\sim 0.25 \text{ mm}^2$   $1 \text{ }\mu\text{m}$ -thick membrane was etched in the center of the chip with hydrofluoric acid, a  $\sim 500 \text{ nm}$  pore was then bored in the center of the membrane with a focused ion beam (FEI Nova 600 Nanolab DualBeam SEM/FIB). [11] The LFA detection system is illustrated in Figure 6.2. First, a platinum foil electrode soldered with silicon wire was placed in the center of the backing card, and two pieces of Fusion 5 membrane (15 mm in length, 3 mm in width, and 0.37 mm in thickness) were placed on either side of the platinum electrode, leaving a gap of  $\sim 1 \text{ mm}$  between them. Two PDMS strips of about the same thickness as the Fusion 5 membrane were aligned parallel with the membrane on the backing card to prevent leakage. Since the Fusion 5 membrane has a large pore size such that PNA-beads can move through it, PNA-beads were preloaded on the Fusion 5 membrane just upstream of the gap. [12] One thinner PDMS O-ring ( $\sim 100 \text{ }\mu\text{m}$  in thickness) was attached to the smooth backside (opposite to the etched well) of the glass chip to protect the nanopore, and another thicker PDMS O-ring ( $\sim 500 \text{ }\mu\text{m}$  in thickness) was attached to the other side of the glass chip to serve as the reservoir. The glass chip with the smooth backside face down was then placed on top of the membrane assembly with the nanopore positioned directly above the gap. One Ag/AgCl pellet electrode was placed in the PDMS reservoir on the top side of the chip in a droplet of hybridization buffer. Both electrodes were connected to a multichannel potentiostat. After setting up the LFA system, we firstly deposited  $10 \text{ }\mu\text{L}$  of extracted RNA sample near the previously deposited PNA beads and allowed the hybridization to occur. After 3 minutes of hybridization,  $100 \text{ }\mu\text{L}$  of extracted RNA sample was injected at the origin of upstream Fusion 5 membrane. As the RNA sample flowed over the PNA-beads by capillary action, the hybridized PNA beads were swept slowly into the gap below the glass chip and



therefore entered the nanopore proximity. A voltage of 1.5 V was applied across the nanopore, and the current over time was recorded. Immediately after the first detection signal (indicated by  $\geq 10$  seconds of sustained ionic current drop) was observed, the polarity of the electronic field was reversed to -1.5 V to attempt to unblock the pore. After  $\sim 20$  seconds of reversed polarity, the field was flipped back to 1.5 V to confirm baseline current recovery and detection signal reproducibility.

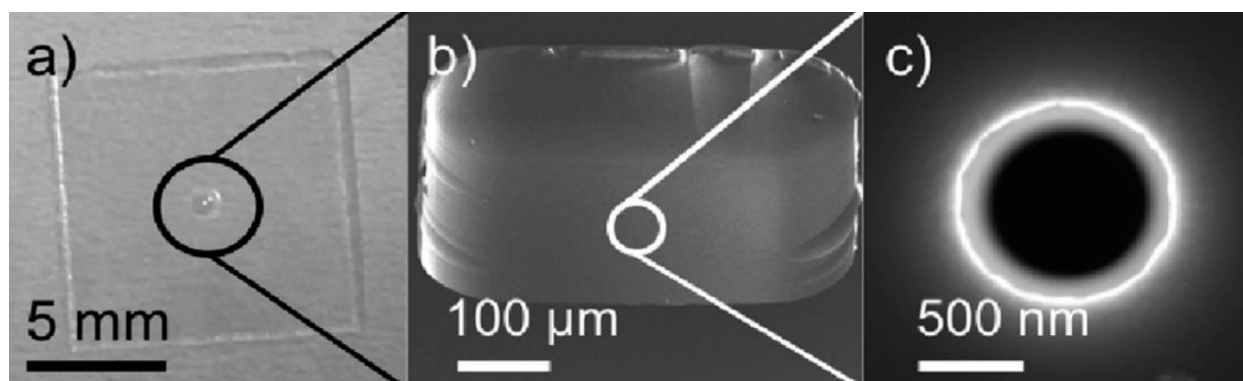


Figure 6.1. a) A microfabricated 1 cm  $\times$  1 cm glass chip. b) SEM image of  $\sim 0.25$  mm<sup>2</sup>, 1  $\mu$ m-thick membrane in the center of glass chip by wet etch. c) SEM image of  $\sim 500$  nm nanopore bored in the center of etched membrane using FIB.[11]

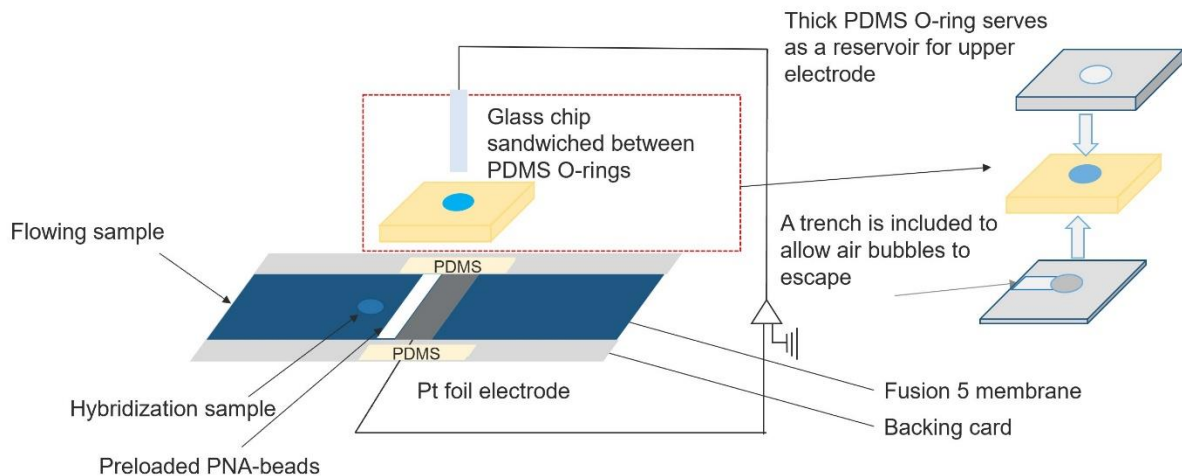


Figure 6.2. Schematic diagram for the lateral flow assay with integrated nanopore detector. Not to scale.

### 6.3 Result and Discussion

The experimental results obtained with our LFA format nanopore detector are summarized in Tables 6.1-6.2 and Figure 6.3. By hybridizing *E. coli* PNA-beads with target *E. coli* 16S rRNA, we successfully demonstrated rapid detection with rRNA samples ranging from 10 fM to 10 aM. Negative controls were performed by hybridizing *E. coli* PNA-beads with *P. putida* RNA, and no false positives were observed for over 1000 seconds. This indicated that the limit of detection (LOD) of the LFA detector is about 10 aM. In a more realistic simulation of pathogen rRNA detection, we conducted tests with samples generated by mixing *E. coli* RNA with a 1000-fold greater amount of *P. putida* RNA. The results also showed rapid detection at 10 aM with no false negatives, which indicated that our LFA format nanopore detector can selectively detect target RNA against a higher concentration of off-target RNA.

Our LFA format nanopore detector also achieved great success in total assay time. By preloading the PNA-beads on the lateral flow chip and forming a compact-bed structure, better interfacial contact between PNA beads and flowing target rRNA was established and therefore

better hybridization efficiency was achieved. This also avoided the time-consuming external sampling and centrifuging steps. In this process, since buffer dried out with preloaded PNA beads on the Fusion 5 membrane prior to use, maximum concentration of electrolyte was found near the gap as the RNA sample flowed through. As diffusion occurred, the electrolyte concentration near the pore proximity decreased over time and thereby caused a current drift at the beginning. In addition to the hybridization efficiency, the detection time was shortened by reducing the travel distance from PNA-beads bound with target RNA to the nanopore. The first detection event, indicated by first sustain ionic current drop, for most cases occurred in around 100 seconds. One additional reversibility check was done by temporarily reversing the voltage polarity, which drove the PNA-beads with hybridized target RNA away from the pore. The detection signal was subsequently confirmed by resumption of the baseline operating voltage. Note that the reversibility check in some cases took a few hundred seconds to complete, and we hypothesize that PNA-beads with hybridized target RNA were embedded in the Fusion 5 membrane after reversing the voltage polarity, which inhibited movement of the hybridized PNA-beads conjugates back to proximity with the nanopore. This issue could be addressed by increasing the voltage. Including the three minutes of hybridization time, the total assay time for our LFA format detector is anywhere from 5 to 15 minutes, which is remarkable for this easily assembled POC prototype that does not rely on NA amplification.

Similar to previous work, transient drops in ionic current were observed in some tests, and we hypothesized this is due to the approach of PNA-beads with nonspecifically bound, negatively charged species to the nanopore where the weakly bound species were removed in the strong electric field and the PNA-beads subsequently were swept away by the opposing electroosmotic flow. [10, 11, 13, 14] At around neutral pH, silanol groups on the glass surfaces deprotonate giving

rise to a layer of fixed negative charges. Cationic counterions form a second layer of mobile positive charges. The movement of these hydrated cations toward the cathode results in an electroosmotic flow that exerts a drag force on beads carrying negative charge moving in the opposite direction. This active mechanism to avert false positives is a unique aspect of our nanopore detection system.

To better illustrate the potential clinical applicability of our LFA format detector, tests with 10 CFU/mL of *E. coli* against  $10^6$  CFU/mL of *P. putida* were also performed. The concentration of 10 CFU/mL was chosen to ensure that at least one viable cell existed for each milliliter of sample processed. The results were in agreement with the tests conducted with extracted RNA. It was notable that our current LOD of 10 attomole was 10 times lower (worse) than our previous record with the Teflon chambers setup.[11] Based on our observations, a portion of the beads dried on the Fusion 5 membrane were retained after flow through of sample. As the sample concentration decreased, less PNA-beads were bound to target RNA, and therefore the bead retention issue became a more significant factor affecting LOD. Since a viable bacterial cell typically contains  $\geq 10,000$  copies of 16S rRNA, 10 attomoles of 16S rRNA corresponds to less than 10 CFU/mL. [9, 15] Therefore, successful detection of 10 aM 16S RNA is still competitive in clinically relevant POC application. In future work, we anticipate resolving the beads retention issue by freeze-drying the PNA-beads in the gap between the two Fusion 5 membranes.

Table 6.1. Summary of results where *E. coli* PNA-beads were hybridized separately with *E. coli* RNA (target) and *P. putida* RNA (negative control)

Target <i>E. coli</i>			Control <i>P. putida</i>		
Concentration		Drop/reversibility	Concentration		Drop/reversibility
10 fM	1	Yes/R	10 fM	1	No
	2	Yes/R		2	No**
	3	Yes/R		3	No
100 aM	1	Yes/R*			
	2	Yes/R			
	3	Yes/R			
10 aM	1	Yes/R*			
	2	Yes/R			
	3	Yes/R			

Yes/R\* Reversibility check took approximately 100 - 300 seconds more than typical  
 No\*\* Transient drop was observed

Table 6.2. Summary of results where *E. coli* PNA-beads were hybridized with mixed *E. coli* and *P. putida* RNA; and where *E. coli* PNA-beads were hybridized with RNA extracted from mixtures of cultures of *E. coli* and *P. putida*

10 aM <i>E. coli</i> + 10 fM <i>P. putida</i>		10 CFU/mL <i>E. coli</i> + 10 <sup>6</sup> CFU/mL <i>P. putida</i>	
	Drop/reversibility		Drop/reversibility
1	Yes/R	1	Yes/R
2	Yes/R	2	Yes/R*
3	Yes/R*	3	Yes/R

Yes/R\* Reversibility check took approximately 100 - 200 second more than typical

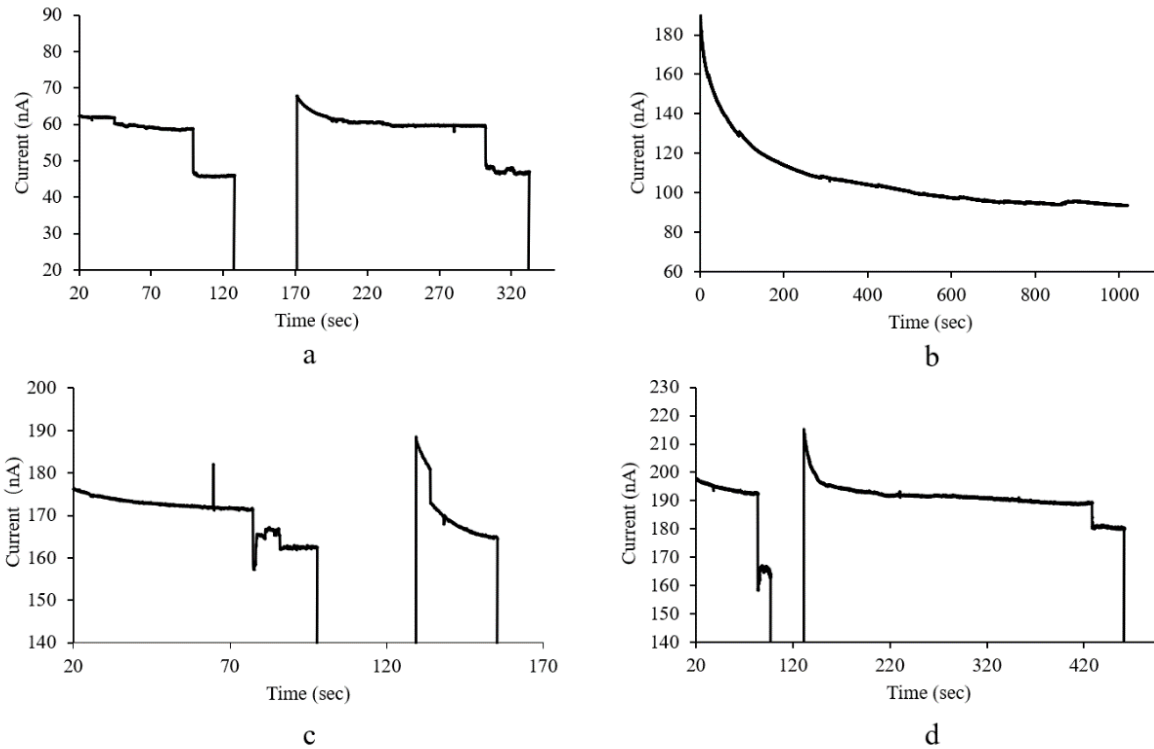


Figure 6.3. PNA-bead tests with LFA format nanopore detector: a) Repeated, consistent current drops for *E. coli* PNA-beads hybridized with 10 aM of target *E. coli* 16S rRNA, b) No current drop for *E. coli* PNA-beads hybridized with 10 fM control *P. putida* 16S rRNA, c) Repeated, consistent current drops for *E. coli* PNA-beads hybridized with 10 aM of *E. coli* 16S rRNA against 10 fM control *P. putida* 16S rRNA, and d) Repeated, consistent current drops for *E. coli* PNA-beads hybridized with RNA extracted from a mixture of 10 CFU/mL of *E. coli* and  $10^6$  CFU/mL of *P. putida*.

## 6.4 Conclusion

A novel nanopore detector was successfully integrated with the LFA format. This LFA format nanopore detector was successfully used to detect *E. coli* 16S rRNA at 10 aM and *E. coli* in culture at 10 CFU/mL. No false positives were observed with 100 fM of *P. putida* RNA or with *P. putida* cells. This integrated diagnostic testing process was accomplished within 15 mins. These results suggest that this rapid and potentially inexpensive technology may one day prove advantageous for POC use. Indeed, with further integration of cell lysis and RNA extraction, this

simple, amplification-free detection technology may lead to inexpensive, rapid POC pathogen detection devices with minimal reagent requirements.

## 6.5 Reference

1. Cristillo, A.D., et al., *Point-of-Care Sexually Transmitted Infection Diagnostics: Proceedings of the STAR Sexually Transmitted Infection-Clinical Trial Group Programmatic Meeting*. Sex Transm Dis, 2017. **44**(4): p. 211-218.
2. Niemz, A., T.M. Ferguson, and D.S. Boyle, *Point-of-care nucleic acid testing for infectious diseases*. Trends Biotechnol, 2011. **29**(5): p. 240-50.
3. Atkinson, L.M., et al., *'The waiting game': are current chlamydia and gonorrhoea near-patient/point-of-care tests acceptable to service users and will they impact on treatment?* Int J STD AIDS, 2016. **27**(8): p. 650-5.
4. Hsieh, Y.H., et al., *Perceptions of an ideal point-of-care test for sexually transmitted infections--a qualitative study of focus group discussions with medical providers*. PLoS One, 2010. **5**(11): p. e14144.
5. Cao, Y., Z. Zheng, and H.G. Monbouquette, *Nucleic acid amplification-free detection of DNA and RNA at ultralow concentration*. Curr Opin Biotechnol, 2021. **71**: p. 145-150.
6. Bishop, J.D., et al., *Sensitivity enhancement in lateral flow assays: a systems perspective*. Lab Chip, 2019. **19**(15): p. 2486-2499.
7. Huang, D., et al., *Microfluidic Ruler-Readout and CRISPR Cas12a-Responded Hydrogel-Integrated Paper-Based Analytical Devices (muReaCH-PAD) for Visible Quantitative Point-of-Care Testing of Invasive Fungi*. Anal Chem, 2021. **93**(50): p. 16965-16973.
8. Fridley GE, H.C., Oza SB, Yager P, *The evolution of nitrocellulose as a material for bioassays*. MRS Bulletin, 2013. **38**: p. 326–330.

9. Stender, H., et al., *Rapid detection, identification, and enumeration of Escherichia coli cells in municipal water by chemiluminescent in situ hybridization*. Appl Environ Microbiol, 2001. **67**(1): p. 142-7.
10. Esfandiari, L., et al., *PCR-Independent Detection of Bacterial Species-Specific 16S rRNA at 10 fM by a Pore-Blockage Sensor*. Biosensors (Basel), 2016. **6**(3).
11. Koo, B., et al., *Amplification-free, sequence-specific 16S rRNA detection at 1 aM*. Lab Chip, 2018. **18**(15): p. 2291-2299.
12. Ruiz-Vega G, K.M., Pellitero MA, Baldrich E, del Campo FJ., *Electrochemical Lateral Flow Devices: Towards Rapid Immunomagnetic Assays*. ChemElectroChem, 2017. **4**(4): p. 880-889.
13. Esfandiari, L., et al., *Sequence-specific DNA detection at 10 fM by electromechanical signal transduction*. Anal Chem, 2014. **86**(19): p. 9638-43.
14. Esfandiari, L., H.G. Monbouquette, and J.J. Schmidt, *Sequence-specific nucleic acid detection from binary pore conductance measurement*. J Am Chem Soc, 2012. **134**(38): p. 15880-6.
15. Janda, J.M. and S.L. Abbott, *16S rRNA gene sequencing for bacterial identification in the diagnostic laboratory: pluses, perils, and pitfalls*. J Clin Microbiol, 2007. **45**(9): p. 2761-4.



## Chapter 7: Recommendations for future work

Recall that the ideal point-of-care application should be simple, fast, and robust. We still have some aspects to improve to meet these criteria.

### 7.1 Cell lysis

Rapid commercial RNA extraction kits are not ideal for POC application, because multiple stages of washing and elution are still involved. It is thereby important for us to investigate a more efficient path to process the RNA extraction and cleanup. It is still encouraged to optimize the lipase treatment since it has been tested successfully under certain condition. A study demonstrated that a high pH lipase could be produced by *Staphylococcus* sp. Stain, and this lipase have been shown with high activity at pH 12. [1] So, in the future we might be able to incorporate small amount of this lipase into our alkaline lysis mixture. Research has also pointed out that multiple ribonuclease (RNases) with optimal alkaline pH are present in human urine, and these RNases could potentially degrade the target RNA.[2] Nonionic surfactant (*i.e.*, Triton X100 or TWEEN 80), reducing reagent (*i.e.*, dithiothreitol or DTT), and carrier RNA could be applied with the alkaline solution to enhance the lysing efficiency and stabilize the extracted RNA.[3] The nonionic surfactant could disrupt the normal architecture of the lipid bilayer and reduce the surface tension of the cell membrane, DTT could covalently destroy the disulfide bonds of the RNases and therefore deactivate the RNases, and carrier RNA could also act as an inhibitor to RNases. In addition, nonionic surfactant could be a potential alternative solution to the lipid/phospholipids in urine issue, because these surfactants could potentially break a large lipid aggregation into smaller micelles that would pass through the nanopore.[4]

## 7.2 Develop a syringe type device for NA extraction

To eliminate pipetting and centrifugation steps, it is also encouraged to develop a simple all-in-one device for cell lysis and RNA extraction. Since our target LOD is about 10 CFU/mL, it is necessary to start with 1 mL of sample. However, given that there are  $\geq 10,000$  copies of rRNA per viable bacterial cell, we can process a much smaller amount of the lysed sample onto our LFM detector in practice. One proposed syringed device is illustrated in Figure 7.1. The syringe will be preloaded with dry lysis buffer and about 1 mL of sample is drawn up through a check valve and through one arm of the Y connector to the lysis buffer in the syringe barrel. After 1 min,  $\sim 100 \mu\text{L}$  of lysed sample is pushed through the other arm of the Y connector and through the filter onto our lateral flow membrane. With such device, anyone without specialized training will be able to operate it within minutes. Since we will work with moderately alkaline solution, neutralization buffer (*e.g.*, Tris-HCl) will be dried on the membrane just downstream of the sample placement area.

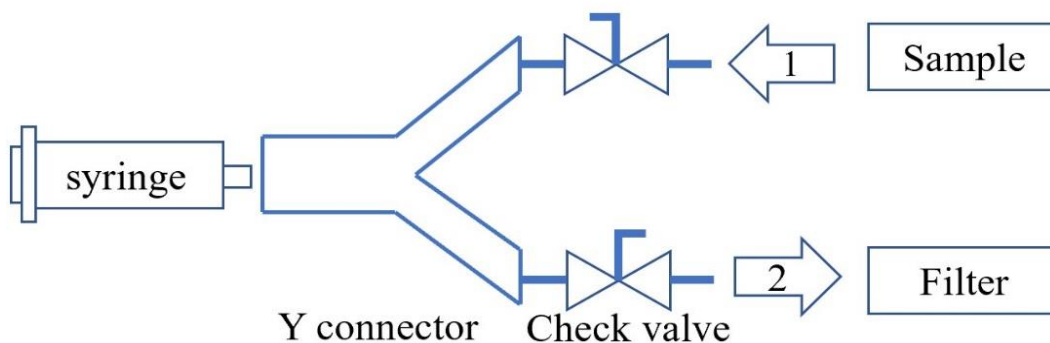


Figure 7.1 Proposed scheme for all-in-one cell lysis device

### 7.3 Improve the LOD and stability

In our first prototype of the LFM format detector, bead immobilization in the Fusion 5 membrane became an issue leading to difficulty in achieving an LOD of 1 aM 16S rRNA. To avoid bead retention, a 3-D printed plastic cartridge, illustrated in Figure 7.2, will be used to replace the original backing card to better enclose the system. The depth of both channels 1 will be designed to be the same as the membrane thickness so that lateral flow membrane strips can be fitted in these channels. Channel 2 will be 1 mm in width (same as original gap) but slightly deeper than channel 1 so that polystyrene PNA-beads can be preloaded into channel 2 prior to the usage. A new membrane with smaller pore size than the 1  $\mu\text{m}$  dia. polystyrene beads will be proposed for future work to avoid any bead embedding issue during the reversibility check (*e.g.*, Whatman Standard 14 from Cytiva). Plastic clips will be used to secure the glass chip onto the cartridge. With such a proposed design, hybridized PNA-beads will be restricted in channel 2 during the detection, and our target LOD of 100 zM 16S rRNA may be approachable.

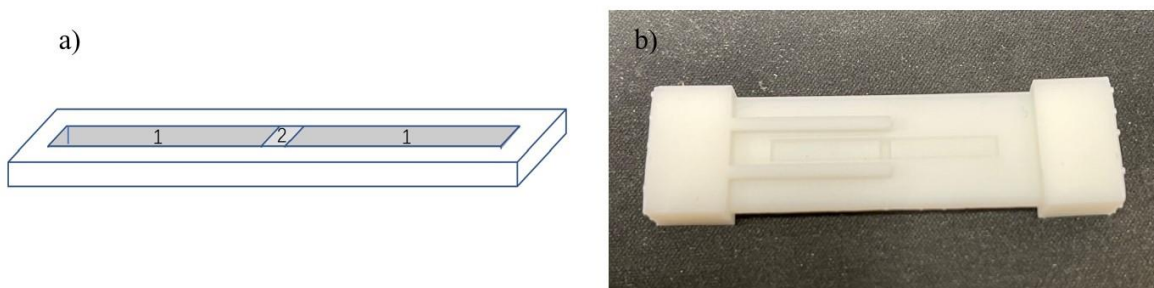


Figure 7.2 a) Proposed cartridge to replace the backing card, not to scale b) 3-D printed cartridge with plastic clips

## 7.4 References

1. Cherif, S., Mnif, S., Hadrich, F. et al. *A newly high alkaline lipase: an ideal choice for application in detergent formulations*. *Lipids Health Dis*, 2011. 10, 221
2. Sugiyama, R.H., A. Blank, and C.A. Dekker, *Multiple ribonucleases of human urine*. *Biochemistry*, 1981. **20**(8): p. 2268-74.
3. Rogacs, A., Y. Qu, and J.G. Santiago, *Bacterial RNA extraction and purification from whole human blood using isotachopheresis*. *Anal Chem*, 2012. **84**(14): p. 5858-63.
4. Lichtenberg, D., H. Ahyayauch, and F.M. Goni, *The mechanism of detergent solubilization of lipid bilayers*. *Biophys J*, 2013. **105**(2): p. 289-99.

## Appendix A: PNA-beads preparation

1. Wash 1  $\mu\text{L}$  of stock bead solution three times in MES buffer. With each wash, spin down the beads in a microcentrifuge at 14,000 RPM for 15 minutes and remove the supernatant.
2. Resuspend the beads in 600  $\mu\text{L}$  MES buffer. Add 23 mg 1-ethyl-3-(3-dimethylaminopropyl)carbodiimide (EDC) to make 200 mM EDC in MES. Incubate the beads for 15 minutes at 50  $^{\circ}\text{C}$ .
3. Add 11.4  $\mu\text{L}$  aliquoted PNA (100  $\mu\text{M}$ ) and incubate for 2 hours at 50  $^{\circ}\text{C}$ .
4. Add 22 mg methoxypolyethylene glycol amine (mPEG-amine). Incubate for one hour at 50  $^{\circ}\text{C}$ .
5. Add 5  $\mu\text{L}$  ethanolamine. Incubate for one hour at 50  $^{\circ}\text{C}$ .
6. Wash beads three times in 0.4x SSC buffer. Resuspend in 400  $\mu\text{L}$  0.4x SSC.
7. Remove 100  $\mu\text{L}$  and wash once in potassium chloride buffer for use in Zetasizer
8. Clean the remaining 300  $\mu\text{L}$  bead solution once in hybridization buffer. Resuspend in 400  $\mu\text{L}$  hybridization buffer for storage.

## **Appendix B: Cell culturing and counting**

### **B.1 Culture *E. coli* and *P. putida***

1. Suspend the lyophilized preparations in soy (*E. coli*) and nutrient (*P. putida*) media, respectively, followed by incubation of days. *E. coli* subsequently was cultured in shake flasks at 37 °C and 250 rpm, and *P. putida* at room temperature and 250 rpm.
2. Store the initiated culture at -80 °C to serve later as inocula.
3. Measure 3 mL of soy media for *E. coli* and 3 mL of nutrient media for *P. putida*.
4. Stab a small portion of frozen culture with a pipette and pipette up and down in the culturing media
5. Culture *E. coli* at 37 °C and 250 rpm, and *P. putida* at room temperature and 250 rpm overnight.

### **B.2 Count viable *E. coli* and *P. putida***

1. Put 1 mL concentrated cells into tube 1
2. Add 900 µL sterile DI water to tube 2-9
3. Take 100 µL concentrated cells, add to tube 2, then take 100 µL of that and add to tube 3 etc.
4. Remove 100 µL from each tube and transfer to Agar plate.
5. Use glass bead to spread the liquid sample evenly on Agar plate.
6. Culture overnight and count the colonies on Agar plate.
7. Multiply the measured cfu by 10 to get the total number of bacteria in the tubes.
8. Culture in tubes 2-9 serve as the stock for future dilution.

### **B.3 Culture and count *N. gonorrhoeae***

1. Subculture a frozen stock of ATCC strain 43069 onto chocolate agar.
2. Agar plates were incubated at 35C with 5% CO<sub>2</sub> for 16-18 hours.
3. Created a 0.5 McFarland of *N. gonorrhoeae*, which represents  $1.5 \times 10^8$  CFUs/ml.
4. Transfer 10 $\mu$ L of sample above into 9990 uL of 0.85% saline to create 150,000 CFU/mL stock.

## **Appendix C: Spike sterilized pool human urine with bacterial culture**

### **C.1 *E. coli* and *P. putida***

1. Transfer 10 µl of the stock (described in Appendix B.2) in 9990 µl human urine to create a final concentration from 10 CFU/mL to 1000 CFU/mL.

### **C.2 *N. gonorrhoeae***

1. Transfer 10µl of the stock (described in appendix B.3) into 9990 µl of commercial urine to create 150 CFUs/ml.
2. Transfer 666 ul of this into 9.333 mL of urine to create a final 10.0 CFU/ml



## Appendix D: RNA extraction

### D.1 Qiagen RNeasy (Chapter 2)

1. Pipette 1.7 mL of *E. coli* or *P. putida* culture into individual, sterile 2 mL microcentrifuge tubes. Spin down (max speed for 1 min) and remove supernatant. First pour out supernatant, then use a pipette to remove any remaining liquid. Make sure not to disturb cell pellet.
2. Lyse the cells. For each pellet, add 200  $\mu\text{L}$  TE lysozyme + 20  $\mu\text{L}$  proteinase K. Resuspend by pipetting up and down a few times. Vortex for 10 sec. Let incubate at 37 °C for at least 45 minutes. Does not have to be on a shaker. Lysed cells will appear clear/transparent.
3. Prepare RLT buffer. Remove 6 mL RLT buffer, mix with 60  $\mu\text{L}$  b-mercaptoethanol (or, if doing fewer than 8 tubes, however much you need at a ratio of 10  $\mu\text{L}$  b-mercaptoethanol to 1 mL RLT buffer). Add 700  $\mu\text{L}$  of this to each tube. Vortex, then spin down at max speed for 2 min.
4. Remove all supernatant and place into new tubes.
5. Into each tube, add 500  $\mu\text{L}$  200 proof ethanol. Precipitation may form, but do not centrifuge. Pipette up and down gently.
6. Spin down 700  $\mu\text{L}$  at a time supernatant into column (30 sec at max speed). Discard flow through.
7. Add 700  $\mu\text{L}$  RW1 buffer, let it flow through column (30 sec at max speed). Discard flow through.
8. For new RPE buffer, add 4 volumes ethanol to 1 volume RPE (44 mL to 11 mL to make 55 mL total). Replace collection tube with a new one. Add 500  $\mu\text{L}$  RPE to column, let spin through (30 sec at max speed).
9. Add another 500  $\mu\text{L}$ , let spin through (2 min at max speed).

10. Decant flow through, let spin for another 1 min at max speed.
11. Transfer column to new 1.5 mL tube (with the cap), add 50  $\mu$ L RNase free water to elute RNA. Make sure to pipette right into the middle of the membrane. Spin for 1 min at max speed to elute. Add another 50  $\mu$ L RNase free water to elute again.
12. Measure RNA concentration and purity with the Nanodrop.

#### **D.2.1 Alkaline Extraction (cell pellet, Chapter 2)**

1. Collect 1 mL culture sample, Spin down (max speed for 1 min) and remove supernatant. First pour out supernatant, then use a pipette to remove any remaining liquid. Make sure not to disturb cell pellet.
2. Add 200  $\mu$ L 0.1M NaOH, mix and let rest at room temperature for 1 minute to lyse the cells
3. Add 400  $\mu$ L of 0.2M Tris-HCl (to bring pH to ~8-8.5) and mix for 10 sec to stop the lysis.
4. Transfer lysed sample into Vivaspin 2 (300,000 MWCO, polycarbonate housing, polyethersulfone membrane), spin down at 1000 rpm for 10 mins
5. Collect filtrate (RNA preparation) and set aside
6. Measure RNA concentration and purity with the Nanodrop.

#### **D.2.2 Alkaline Extraction (urine sample, Chapter 3)**

1. Collect 1 mL urine sample from *Appendix C.1*.
2. Add 2 mL 0.2M NaOH, mix and let rest at room temperature for 1 min
3. Remove 150  $\mu$ L of mixture above and add 300  $\mu$ L of 0.5M Tris-HCl (to bring pH to ~7) and mix for 10 sec.

### **D.3 Direct-zol RNA extraction Kit**

1. [For pelleted cells] Add 300  $\mu$ L of TRI Reagent<sup>®</sup> into pelleted cells and incubate for 5 minutes.
2. [For urine sample] Add 3 mL of the TRI Reagent<sup>®</sup> into 1mL of urine sample and incubate for 5 minutes.
3. Add an equal volume ethanol (95-100%) to a sample lysed in TRI Reagent<sup>®</sup> or similar1 and mix thoroughly.
4. Transfer the mixture into a Zymo-Spin<sup>™</sup> IC Column2 in a Collection Tube and centrifuge at 14000 rpm for 1 minute
5. Transfer the column into a new collection tube and discard the flow-through.
6. Add 400  $\mu$ l Direct-zol<sup>™</sup> RNA PreWash5 to the column and centrifuge. Discard the flow-through and repeat this step.
7. Add 700  $\mu$ l RNA Wash Buffer to the column and centrifuge for 1 minute to ensure complete removal of the wash buffer. Transfer the column carefully into an RNase-free tube (not included).
8. To elute RNA, add 30  $\mu$ l of DNase/RNase-Free Water directly to the column matrix and centrifuge.

## Appendix E: Kinetically Enhanced Hybridization

1. Transfer 600  $\mu\text{L}$  of PNA-conjugated beads in hybridization buffer (10 mM NaCl, 25 mM Tris-HCL, pH 7) to Vivaspin 2 and spin at 1000 rpm for 5 mins, discard filtrate. This step deposits ~2 layers of beads on the filter surface.
2. Transfer RNA prep described in Appendix D to same Vivaspin 2 with filtered beads, spin at 1000 rpm for 5 mins and discard filtrate. Hybridization occurs in this step.
3. Add 600  $\mu\text{L}$  of 0.4X SSC buffer (60 mM NaCl, 6 mM trisodium citrate, 0.01% Tween-80, pH 8) into same Vivaspin as in step #3, spin at 1000 rpm for 5 mins and discard filtrate. This step is used to wash the beads before transfer to testing buffer.
4. Add 600  $\mu\text{L}$  of testing buffer (10 mM KCl, 5.5 mM HEPES, 0.01% Tween-80, pH 7) into same Vivaspin as in step #4, spin at 1000 rpm for 5 mins and discard filtrate. This step is to wash with testing buffer.
5. Add 200  $\mu\text{L}$  testing buffer, sonicate for 1 min, reverse spin at 1000 rpm for 5 min and collect hybridized beads in ~200  $\mu\text{L}$ . Reverse spin removes beads from the filter membrane surface.

## Appendix F

### F.1 Lateral flow strip assembly

1. Cut A-4 size Fusion 5 membrane sheet from Cytiva into  $1.5\text{ cm} \times 3\text{ cm}$  strips.
2. Use a paper cutter to cut the Cytiva backing card into  $1.5\text{ cm} \times 8\text{ cm}$  pieces.
3. Cut the Pt-foil into  $2\text{ mm} \times 1\text{ cm}$  small strips and solder a wire on the end to make a Pt-foil electrode.
4. Peel off the film on the backing card and attach a soldered Pt-foil electrode in the middle of the backing card.
5. Attach two Fusion 5 membrane pieces on top of edges of the foil electrode and the backing.

A less than 1 mm gap is left between these two Fusion 5 membrane pieces to expose the Pt-foil electrode underneath. We call this assembled card the lateral flow membrane strip, shown in Figure 1.

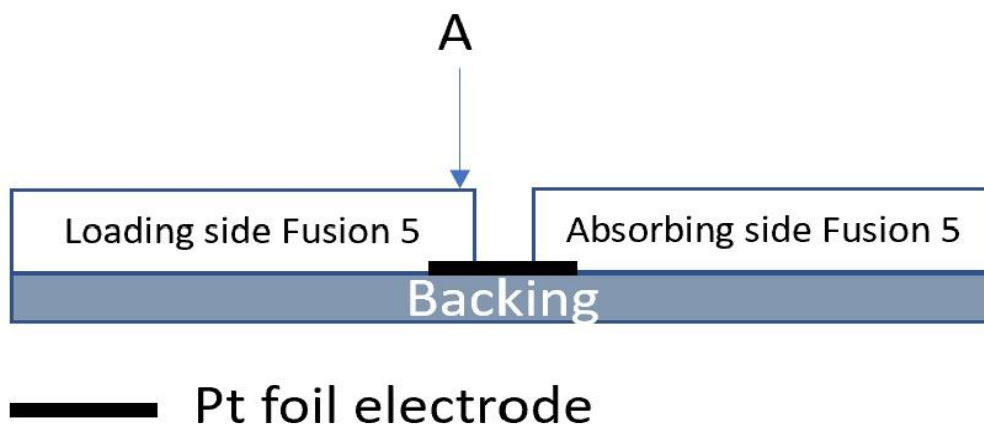


**Figure F.1.** Lateral flow membrane strip, not to scale. Point A is where PNA-modified beads are loaded and dried (see below).

6. Mark one side of the chip to be the loading side.

7. Wash PNA/PEG/ethanolamine-modified polystyrene beads with hybridization buffer (10 mM NaCl, 25 mM Tris-HCL, pH 7, 1% Tween 20).
8. Concentrate the beads by centrifuge filtration and load the beads next to the gap, shown as point A in Figure 1
9. Before the beads get dried, apply vibration force to the beads by holding the lateral flow membrane strip to the wall of a bath sonicator. This step helps prevent bead aggregation.
10. Let the beads dry

## F.2 Glass chip assembly

11. As shown in Figure 2, we sandwich a glass chip with a  $\sim 1 \mu\text{m}$  - 800 nm diameter “nanopore” (must be smaller than bead diameter used) in the middle with two PDMS O-ring shaped films. Cellophane tape (e.g., Scotch tape) was used to briefly remove the dust on PDMS, and this will ensure good attachment to the glass chip.

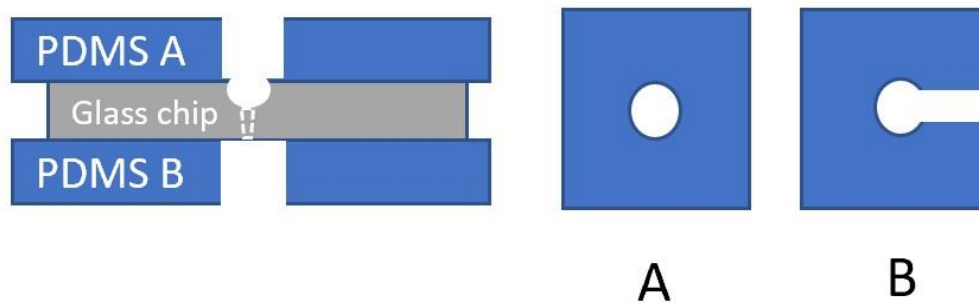


**Figure F.2.** Glass chip with PDMS films attached, not to scale.

12. The bottom PDMS B film is  $\sim 0.3$  mm thick and with a circular opening to expose the nanopore. A channel is carved all the way from the edge to the center. This design enables air to escape when the underlying Fusion 5 membrane is wetted (see below) and prevents the formation of bubbles. The top PDMS A has  $\sim 1$  mm thickness and it also has a circular

opening to expose the nanopore. This circular opening acts as a buffer reservoir for the top electrode that is used in detection (see below).

### F.3 Whole system assembly

13. Attach the lateral flow membrane strip to the potentiostat by using one Ag/AgCl electrode as both counter and reference electrode, while using the Pt-foil electrode as the working electrode.
14. Put the glass chip assembly on the top of the lateral flow membrane strip. Position the nanopore right on top of the gap in the lateral flow membrane strip.

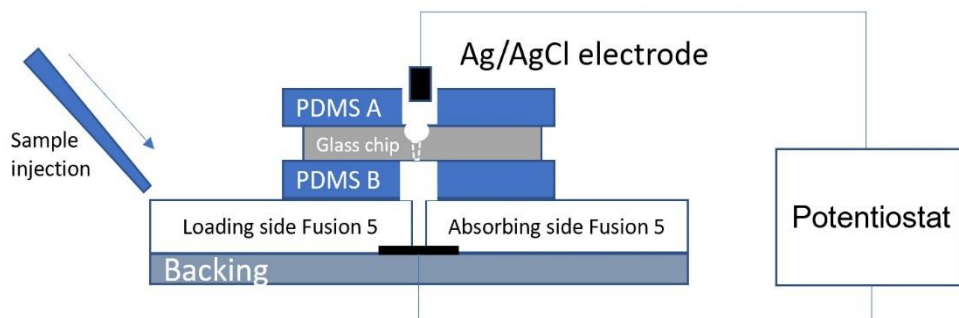


**Figure F.3.** Detection system, not to scale

15. Put a droplet of hybridization buffer in the opening of the top PDMS A of the glass chip assembly.
16. Gently lower the Ag/AgCl electrode mentioned above into the top buffer reservoir in PDMS A also mentioned above to establish an electrical connection through the pore in the glass chip.

#### **F.4 Detection**

17. Deposit ~400  $\mu\text{L}$  of our testing sample onto the loading side of the Fusion 5 membrane.

Due to capillary flow, the liquid sample will flow over the beads so that the target RNA or DNA in the sample will hybridize with the PNA probe on our modified beads. The beads move more slowly in the Fusion 5 membrane than the fluid but at least some get carried into the gap below the pore in the glass chip. Fluid will pass through the gap and to the absorbing side of the Fusion 5 membrane. Fluid also will fill the opening in PDMS B below the glass chip, and air will escape through the channel in PDMS B so that bubbles will not form.

18. During this process, the power to the potentiostat is turned on and data is collected using EC-lab software on a computer.

19. A stable baseline current will appear. For a positive test, after ~200 s-800 s, a sustained drop in the current will occur due to the PNA-beads with hybridized target nucleic acid blocking the nanopore, and we take this as our detection signal. For a negative test, there is just a stable baseline current, no drops are observed. Figure 4 shows typical successful detection data.